System Identification of Smart Structures using a Nonlinear WARMA Model

by

JungMi Kim

A Thesis

Submitted to the Faculty

of

WORCESTER POLYTECHNIC INSTITUTE

In Partial fulfillment of the requirements for the

Degree of Master of Science

in

Civil Engineering

By

December 2012

APPROVED:

_____

Professor Yeesock Kim, Thesis Advisor

_____

Professor, Tahar El-Korch, Committee Member

Abstract

System identification (SI) for constructed structural systems has received a lot of attention with the continuous development of modern technologies. This thesis proposes a new nonlinear time series model for use in system identification (SI) of smart structures. The proposed model is implemented by the integration of a wavelet transform (WT) and nonlinear autoregressive moving average (NARMA) time series model. The approach demonstrates the efficient and accurate nonlinear SI of steel smart structures under ambient excitation and reinforced smart structures subjected to high impact loads. To demonstrate the effectiveness of the wavelet-based NARMA modeling (WNARMA), smart structures equipped with magnetorheological (MR) dampers are investigated. The simulation results show that the computation of the WNARMA model is faster than that of the NARMA model without sacrificing the modeling accuracy. In addition, the WNARMA model is robust against noise in the data since it inherently has a denoising capacity.

Acknowledgements

I sincerely thank my advisor and mentor professor Yeesock Kim for his continuous guidance, support, encouragement, and motivation throughout my years of graduate studies. His guidance helped me in all the time of research and writing this thesis. I would also like to thank my committee member, professor El-Korchi for his encouragement, insightful comments and hard questions.

I would like to thank my parents, order brother, and other family members for the love and support they have given me.

Table of Contents

Abstract 2

Acknowledgements 3

List of Tables 5

List of Figures 6

1. Introduction 8

2. Wavelet based nonlinear ARMA (WNARMA) model 11

2.1. Wavelet transform 11

2.2. Nonlinear ARMA model 13

2.3. Wavelet based nonlinear ARMA model 17

3. Case studies 18

3.1. Case study 1 18

3.1.1. Structure equipped MR dampers 18

3.1.2. Modeling 21

3.1.3.Conclusion 41

3.2. Case study 2 41

3.2.1. Experimental setup 42

3.2.2. Data acquisition 45

3.2.3. Modeling 47

3.2.4. Conclusion 68

4. Summary 69

5. Future works 70

6. Reference 71

List of Tables

Table 1. Training Results for NARMA and WNARMA Models 40
Table 2. Obtained H_1-H_5 using the NARMA model from 100 times of the impact tests 65
Table 3. Obtained H_1-H_5 using the WNARMA model from 100 times of the impact tests 66

List of Figures

Figure 1. The Archit ecture of Wavelet Based ARMA 18
Figure 2. Three-story building with MR damper system 19
Figure 3. Comparison of the NARMA with the origianl data with free noise (Case I) 23
Figure 4. Comparison of the NARMA with the origianl data with 10% noise (Case I) 24
Figure 5. Comparison of the NARMA with the origianl data with 20% noise (Case I) 25
Figure 6. Comparison of the NARMA with the original data with 30% noise (Case I) 26
Figure 7. Comparison of the WNARMA with the original data with noise free (Case I) 27
Figure 8. Comparison of the WNARMA with the origianl data with 10% noise (Case I) 28
Figure 9. Comparison of the WNARMA with the original data with 20% noise (Case I) 29
Figure 10. Comparison of the WNARMA with the original data with 30% noise (Case I) 30
Figure 11. Comparison of the WNARMA with the original data with noise free (Case 2) 31
Figure 12. Comparison of the WNARMA with the original data with 10% noise (Case II) 32
Figure 13. Comparison of the WNARMA with the original data with 20% noise (Case II) 33
Figure 14. Comparison of the WNARMA with the original data with 30% noise (Case II) 34
Figure 15. Comparison of the WNARMA with the origial data with noise free (Case III) 35
Figure 16. Comparison of the WNARMA with the original data with 10% noise (Case III) 36
Figure 17. Comparison of the WNARMA with the original data with 20% noise (Case III) 37
Figure 18. Comparison of the WNARMA with the origianl data with 30% noise (Case III) 38
Figure 19. Drop-tower test equipment with a capacity of 22,500 kg 43
Figure 20. Prepared concrete beams 44
Figure 21. Configuration of reinforcement 44
Figure 22. Magnetorheological (MR) damper 45
Figure 23. Configuration of the sensors and data acquisition system 46
Figure 24. Comparison of the NARMA with the original data (best case) 48
Figure 25. Comparison of the NARMA with the original data (best case) 49
Figure 26. Comparison of the NARMA with the original data (best case) 50
Figure 27. Comparison of the NARMA with the original data (best case) 51
Figure 28. Comparison of the NARMA with the original data (worst case) 52

Figure 29. Comparison of the NARMA with the original data (worst case) 53
Figure 30. Comparison of the NARMA with the original data (worst case) 54
Figure 31. Comparison of the NARMA with the original data (worst case) 55
Figure 32. Comparison of the WNARMA with the original data (best case) 56
Figure 33. Comparison of the WNARMA with the original data (best case) 57
Figure 34. Comparison of the WNARMA with the original data (best case) 58
Figure 35. Comparison of the WNARMA with the original data (best case) 59
Figure 36. Comparison of the WNARMA with the original data (worst case) 60
Figure 37. Comparison of the WNARMA with the original data (worst case) 61
Figure 38. Comparison of the WNARMA with the original data (worst case) 62
Figure 39. Comparison of the WNARMA with the original data (worst case) 63
Figure 40. Average and 1-sigma of H_4 (fitting rate) of WNARMA and NARMA models from 100 times of the impact tests (a) 1st acceleration (b) 2nd acceleration (c) strain (d) displacement 67
Figure 41. Average and 1-sigma of H_5 (computation time) of WNARMA and NARMA models from 100 times of the impact tests (a) 1st acceleration (b) 2nd acceleration (c) strain (d) displacement 68

1. Introduction

System identification (SI) for structures has received a lot of attention with the continuous development of modern technologies (Nishitani et al 1996, Takewaki et al 2012, Lei and Wu 2011). Using the SI technique is expected to provide accurate information of the dynamic characteristics of structures. However, constructing a suitable mathematical model for nonlinear structures is one of many difficult problems. Smart structures are considered as one of the nonlinear structural systems. This is because the smart damping devices are highly nonlinear, and when they are employed to the structures, which are generally assumed to behave linearly, the combined system becomes to be nonlinear (Yi et al 1999, Kim et al 2009).

The role of the identification of nonlinear characteristics of structures has attracted a lot attention as the applications of smart structures have been increasing. In recent years, smart structures have been adopted from many engineering fields because they can sense and adapt to its environment dynamically (Fisco and Adeli 2011, Kim et al 2009). In addition, smart structures have been received increasing attention to reduce the impact of structures since a smart control system can provide an effective way to absorb and dissipate the external impact energy on structures in real time. A magnetorheological (MR) damper is one of the smart control devices, and it has been proven to provide high performance under high impact loads from the recent researches (Liu and Chen 2011, Wang and Li 2006, Ahmadian and Norris 2007, Zhang et al 2009). Therefore, the development of an appropriate mathematical model of the structures employing smart damping devices is essential.

SI can be classified as parametric and nonparametric approaches (Bani-Hani et al 1999). Parametric methods are used to determine a finite number of parameters such as structural

stiffness and damping, which are physical quantities of structural systems (Andersen 1997). In order to identify an accurate system model, a sufficient number of modal parameters must be obtained. However, since most of the civil structures show nonlinear behavior, determining these parameters is often very difficult and time consuming process, and it also requires a lot of clean and complete data to identify the actual system (John 1987).

Nonparametric methods can determine infinite number of parameters and estimate model parameters without assuming a parametric model set. Nonparametric methods are able to train data to predict the structural response even though the system model does not represent physical quantities directly. In other words, the system model can be determined even when little information on the system is provided. Therefore, nonparametric methods have great potential to apply SI technique to complex nonlinear structures. It has been extensively researched by various civil engineers (Xu et al 2009, Lei and Wu 2011, Kim et al 2009, Adeli and Jiang 2006, Yun et al 2008, Kerschen et al 2006, Hasiewicz and Pawlak 2000). Furthermore, the nonparametric SI approach is effective for the complex nonlinear problems of large civil structures (Yi et al 1999, Kim et al 2009).

The nonparametric SI approach can either be applied to both input and/or output data. The output data based SI method has become of great significance in assessing engineering structures since the input data is not always available. In general, it is difficult to obtain input data when civil structures, such as offshore structures and bridges, are subjected to uncertain natural excitations such as traffic, wind and waves (Rytter et al 1990, Ren and Zong 2004, James et al 1996, Devriendt et al 2007, Kullaa and Tikkonen 2001). Since the ambient excitation is always present but immeasurable, output only identification under ambient excitation seems to be the most desirable approach. With output only approach, it is possible to identify the dynamic

properties of the system in real operating conditions where the loading conditions are unknown (Devriendt et al 2007). This approach has been successfully applied to structures excited by ambient excitations (Le and Tamura 2009, Brincker et al 2001, Lei et al 2003, Whelan et al 2009, Kim et al 2002, Parloo et al 2003).

The autoregressive moving average (ARMA) time series model is one possible approach of output data based SI methods, and it has been proven to accurately describe the dynamic response of structural systems from various researchers (Silva et al 2008, Nair et al 2006, Ettefagh 2007, Nair and Kiremidjian 2007, Carden and Brownjohn 2007, Brincker et al 1995, Zheng and Mita 2008, Brinker et al 1995, Kondo and Hamamoto 1996). However, most of these models are performed under linear system assumptions. Generally, time series analysis and its applications assume a linear relationship among variables, that is, the forecasted values are assumed to be a function of the previous values (Hogg and Tindale 2008, Silva 2008). Although linear system assumptions are possible to reduce the mathematical complexity of the models, it can also lead to insufficient representations when nonlinear behavior of structures is considered (Song and Wang 1998, Silva 2008). A possible approach to increase the accuracy is to use nonlinear terms. Although it may be challenging to develop an appropriate mathematical model of nonlinear characteristics of structures, it produces more accurate results. In order to modeling characteristics of structures, which have nonlinear behavior, a nonlinear ARMA (NARMA) model was developed (Loh and Duh 1996, Silva 2008, Loh et al 2000, Hunter 1990). However, since the NARMA model requires long computation time to obtain the parameter estimates, it has a limitation when implementing the structural model in real time. By integrating of wavelet transforms (WT), the computation time can be significantly reduced.

The WT provides a time-frequency representation of the signal through time and frequency window functions. The application of the WT has been used for SI due to its advantages (Hou et al 2000, Bajaba and Alnefaie 2005, Rucka 2011, Gokdag 2010). The WT affects reduction of computation time and is also effective in reduction of noise when measured vibration signals are obtained with noise. In this paper, a wavelet based nonlinear ARMA (WNARMA) model is proposed as an integration of the WT to the NAMRA model for identification of nonlinear behavior of structures.

The rest of the paper is organized as follows. Section 2 describes the WNARMA time series model, which includes concepts of the NARMA time series model and the WT. Section 3 provides two case studies; first case study is conducted for SI of a three-story building employing an MR damper under ambient excitation, and for second case study, the experimental study is performed for SI of a reinforced concrete structure employing an MR damper under a high impact load. Section 4 provides the summary of the paper.

2. Wavelet based nonlinear ARMA (WNARMA) model

The WNARMA time series model is proposed to develop the data-driven model. To estimate the parameters of the ARMA model, a least squares which minimizes the prediction error, is used. In order to reduce the computation time, a discrete wavelet transform (DWT) is used for wavelet decomposition.

2.1. Wavelet transform

The continuous wavelet transform (CWT) is a time-frequency analysis method. It allows arbitrarily high localization of high frequency signal features within the given time.

The CWT can be defined as

$$W_{\psi}f(\delta,\varepsilon)=\frac{1}{\sqrt{\delta}}\int_{-\infty}^{\infty}f(n)\psi^{*}(\frac{n-\varepsilon}{\delta})dx \tag{1}$$

where $\psi(n)$ is the wavelet function, so-called mother function, and δ and ε represent the scale and the translation parameter, respectively.

The discrete wavelet transform (DWT), which can yield a fast computation of the CWT, can be derived

$$W_{l,k}=2^{(-\frac{l}{2})}\sum_{l}\sum_{k}x(n)\psi(2^{-l}n-k) \tag{2}$$

where $x(n)$ is the discrete time signal, and l and k represent the scaling factor and the translation factor, respectively.

The DWT can be applied to a wavelet multi-resolution analysis (WMRA). The WMRA is used in order to decompose the signals into primary components at different resolutions. The objective of performing the wavelet decomposition is to provide a means of dividing the acquired signals into groups of subcomponent signals. Thus, the newly acquired signals consist of approximations and details. The approximations are the signals with low frequency components while the details are the signals with high frequency components. The signals represent the fundamental structural response signals, noise signals, and other signals that might be observed only after damage occurrence (Horton et al 2005).

Scaling function $\psi(n)$ and the corresponding wavelet $\varphi(n)$ are defined by the following dilation equations

$$\psi_{l,k}(n) = 2^{(-\frac{l}{2})}\psi(2^{-l}n - k) \tag{3}$$

$$\varphi_{l,k}(n) = 2^{(-\frac{l}{2})}\varphi(2^{-l}n - k) \tag{4}$$

The scaling function acts as a low pass filter and provides an approximation of original series. On the other hand, the corresponding wavelet acts as a high pass filter and provides the detailed information.

2.2. Nonlinear ARMA model

The linear ARMA model is given by

$$r(n) = \sum_{i=1}^{A} \alpha_i r(n-i) + \sum_{j=0}^{B} \beta_j s(n-j) + e(n) \tag{5}$$

where A and B represent the optimal AR and MA model orders, respectively. The term $e(n)$ is considered a noise source or prediction-error term. The parameters α_i and β_j represent to-be-estimated coefficients of the AR and MA terms, respectively. The candidate vectors are the following: $r(n-1)$,…., $r(n-A)$ and $s(n)$,…., $s(n-B)$. These candidate vectors can be arranged as the matrix shown below

$$\begin{matrix} r(0) & s(1) & r(-1) & s(0) & \dots & r(1-A) & s(1-A) \\ r(1) & s(2) & r(0) & s(1) & \dots & r(2-B) & s(2-B) \\ \vdots & \vdots & \vdots & \vdots & \dots & \vdots & \vdots \\ r(n-1) & s(n) & r(n-2) & s(n-1) & \dots & r(n-A) & s(n-B) \\ \vdots & \vdots & \vdots & \vdots & \dots & \vdots & \vdots \\ r(N-1) & s(N) & r(N-2) & s(N-1) & \dots & r(N-A) & s(N-B) \end{matrix} \quad (6)$$

where N is the total number of data points.

In the NARMA model, the matrix can be expanded not only to include projects between the AR terms and MA terms itself, but also the cross products between the AR terms and MA terms as well. The NARMA can be described by

$$r(n) = \sum_{i_1=1}^{A} \alpha_{i_1} r(n-i_1) + \sum_{i_1=1}^{A} \sum_{i_2=i_1}^{A} \alpha_{i_1,i_2}\, r(n-i_1) r(n-i_2) + \cdots$$
$$+ \sum_{i_1=1}^{A} \ldots \sum_{i_i=i_{i-1}}^{A} \alpha_{i_1,\ldots,i_i} r(n-i_1) \ldots r(n-i_i)$$
$$+ \sum_{j_1=0}^{B} \beta_{j_1} s(n-j_1) + \sum_{j_1=0}^{B} \sum_{j_2=j_1}^{B} \beta_{j_1,j_2}\, s(n-j_1) s(n-j_2) + \cdots$$
$$+ \sum_{j_1=1}^{B} \ldots \sum_{j_i=j_{i-1}}^{B} \beta_{j_1,\ldots,j_i} s(n-j_1) \ldots s(n-j_i) + e(n)$$
$$+ \sum_{i_1=1}^{A} \sum_{j_1=0}^{B} c_{i_1,j_1} r(n-i_1) s(n-j_1)$$
$$+ \sum_{i_1=1}^{A} \ldots \sum_{i_i=i_{i-1}}^{A} \sum_{j_1=1}^{B} \ldots \sum_{j_i=j_{i-1}}^{B} c_{i_1,\ldots,i_i,\ldots,j_1,\ldots,j_i} r(n-i_1) \ldots r(n-j_i) s(n$$
$$- j_1) \ldots s(n-j_i) + e(n) \tag{7}$$

With the new candidates of linearly independent vectors, the least squares analysis is performed by

$$r(n) = \tau_g^T \emptyset + e(n) \tag{8}$$

$$\tau_g = [g_0, g_1, g_2, \ldots, g_R]^T \tag{9}$$

where $\emptyset = [\mu_0, \mu_1, \mu_2, \dots, \mu_R]$, and R is the number of selected linearly independent vector. g_i is the coefficient estimate of the ARMA model. The objective is to minimize the equation error, $e(n)$, in the least squares sense using the criterion function defined as follows

$$J_N(\tau_g) = [r(n) - \tau_g^T \emptyset]^2 \tag{10}$$

The criterion function in (6) is quadratic in τ_g, and can be minimized analytically with respect to τ_g, yielding the following equation

$$\left(\widehat{\tau_g}\right) = [\emptyset\emptyset^T]^{-1} \emptyset\, r(n) \tag{11}$$

With the obtained coefficients, calculate every $\overline{g_m^2 \mu_m^2}$, and rearrange the μ_m in descending order. Note that the over-bar represents the time average. At this step of the algorithm, the number of candidate vectors, μ_m, necessary for obtaining proper accuracy needs to be chosen. This approach is taken in order to retain only the μ_m values that reduce the error value significantly. If either negligible decrease or increase in the error value by adding an additional μ_m value is found, then those μ_m values are dropped from the model. Once only those μ_m values that reduce the error value significantly are obtained, the NARMA model terms are estimated using the least squares method (Lu et al 2001). In order to enhance the efficiency of the NARMA model, the WT method is introduced. The Integration of WT method not only helps to reduce the computation time, but also to reduce the amount of noise and the amount of data.

2.3. Wavelet based nonlinear ARMA model

As the WT provides a useful decomposition of the time series for both time and frequency, when it is integrated with the NARMA model, the WT enhances the efficiency of the model in terms of reduction of the computation time and noise. The WNARMA model is proposed as an integration of the WT to NARMA model. The WNARMA can be derived by

$$
\begin{aligned}
r(n) = & \sum_{i_1=1}^{A} a_{i_1} r\psi_{l,k}(n-i_1) + \sum_{i_1=1}^{A}\sum_{i_2=i_1}^{A} a_{i_1,i_2}\, r\psi_{l,k}(n-i_1) r\psi_{l,k}(n-i_2) + \cdots \\
& + \sum_{i_1=1}^{A} \dots \sum_{i_i=i_{i-1}}^{A} a_{i_1,\dots,i_i} r\psi_{l,k}(n-i_1) \dots r\psi_{l,k}(n-i_i) \\
& + \sum_{j_1=0}^{B} b_{j_1} s\psi_{l,k}(n-j_1) + \sum_{j_1=0}^{B}\sum_{j_2=j_1}^{B} b_{j_1,j_2}\, s\psi_{l,k}(n-j_1) s\psi_{l,k}(n-j_2) + \cdots \\
& + \sum_{j_1=1}^{B} \dots \sum_{j_i=j_{i-1}}^{B} b_{j_1,\dots,j_i} s\psi_{l,k}(n-j_1) \dots \psi_{l,k} s(n-j_i) \\
& + \sum_{i_1=1}^{A}\sum_{j_1=0}^{B} c_{i_1,j_1} r\psi_{l,k}(n-i_1) s\psi_{l,k}(n-j_1) \\
& + \sum_{i_1=1}^{A} \dots \sum_{i_i=i_{i-1}}^{A} \sum_{j_1=1}^{B} \dots \sum_{j_i=j_{i-1}}^{B} c_{i_1,\dots,i_i,\dots,j_1,\dots,j_i} r\psi_{l,k}(n-i_1) \dots r\psi_{l,k}(n \\
& - i_i) s\psi_{l,k}(n-j_1) \dots s\psi_{l,k}(n-j_i) + e(n)
\end{aligned}
\tag{12}
$$

Figure 1 shows process of this WNARMA model.

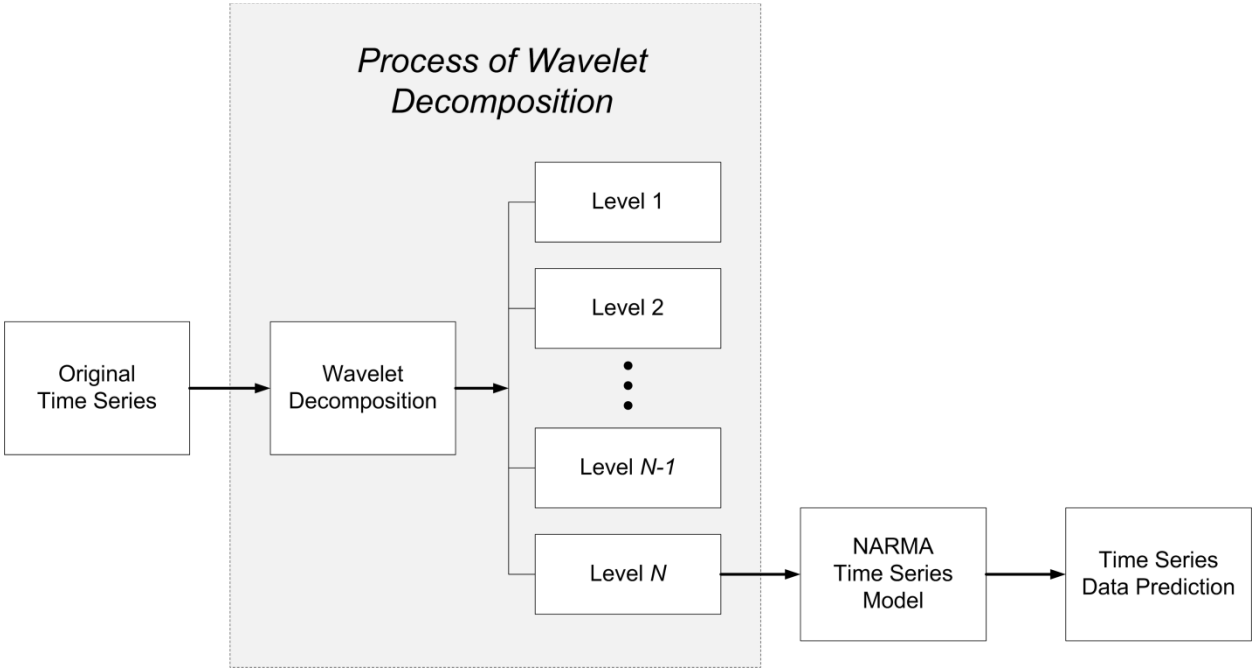

Figure 1. The Archit ecture of Wavelet Based ARMA

3. Case studies

3.1. Case study 1

3.1.1. Structure equipped an MR damper

To demonstrate the effectiveness of the proposed WNARMA model, it is applied to a three-story building employing an MR damper. The MR damper is one of the promising semi-active control devices for structural vibration reduction that combines the best features of both active and passive control systems. The MR damper is filled with MR fluid and controlled by a magnetic field. When the magnetic field is applied to the MR fluid, the MR fluids are changed into a semi-solid state in a few milliseconds. Therefore, the stiffness of the MR damper will be changed

and it reduces an undesired shock or vibration. A typical example of a building structure employing an MR damper is depicted in Figure 2.

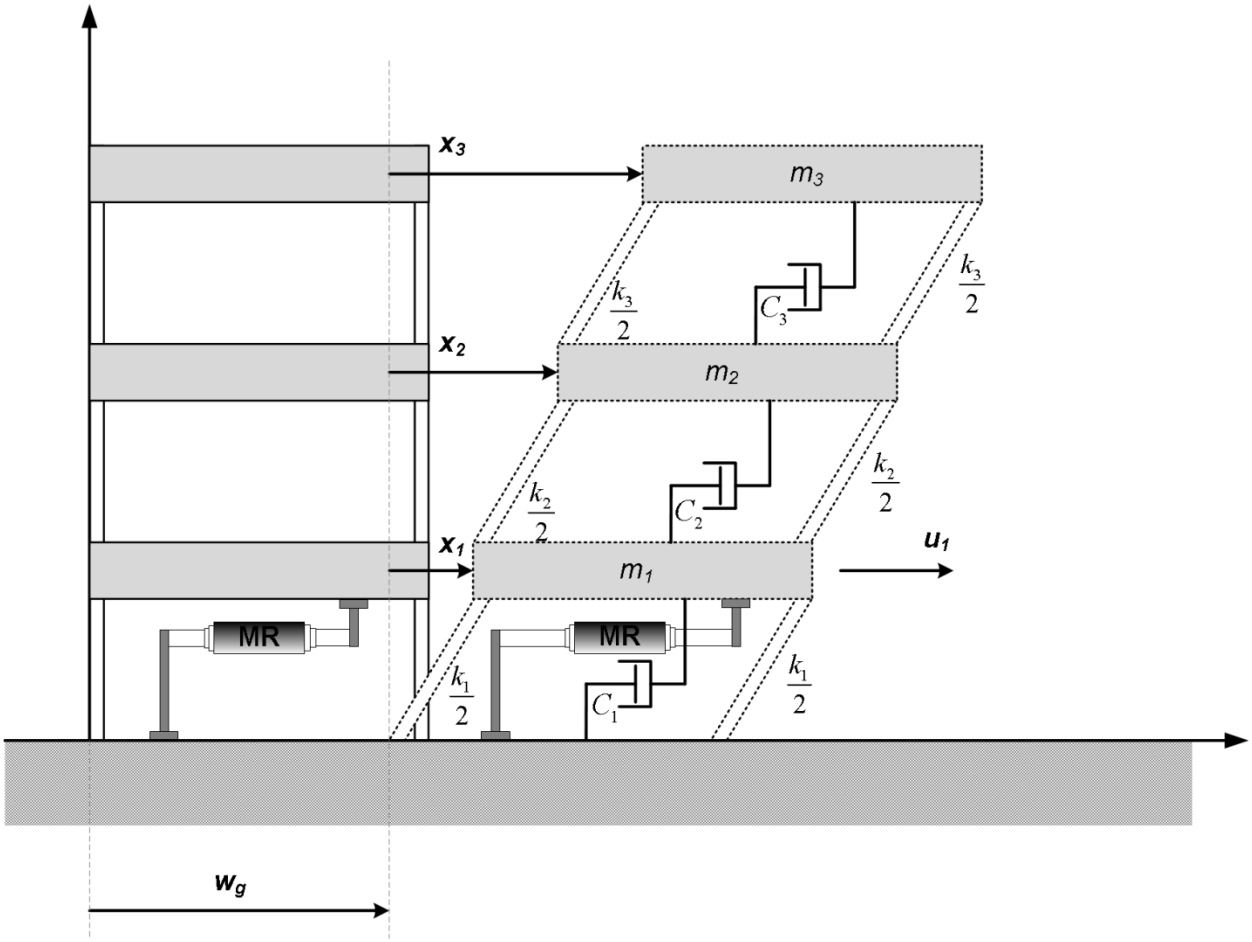

Figure 2. Three-story building with MR damper system

The MR damper can be installed at arbitrary locations within the building. In this structure, the MR damper is connected on the 1st floor. The equation of motion for the structure is defined as

$$\boldsymbol{M}\ddot{x} + \boldsymbol{C}\dot{x} + \boldsymbol{K}x = \Gamma f_{\boldsymbol{MR}}(t, x_i, \dot{x}_i, v_i) - \boldsymbol{M\Lambda}\ddot{w}_g \tag{13}$$

where $\ddot{w}_g$ represents the ground acceleration, $\boldsymbol{M}$ is the mass matrix, $\boldsymbol{K}$ is the stiffness matrix, $\boldsymbol{C}$ is the damping matrix. Vector x is the displacement relative to the ground, $\dot{x}$ the velocity, $\ddot{x}$ the acceleration. x_i and $\dot{x}_i$ are the displacement and the velocity at the i^{th} floor level relative to the ground, respectively. v_i is the voltage level to be applied, and Γ and $\boldsymbol{\Lambda}$ are location vectors of control forces and disturbance signal, respectively. The second order differential equation can be converted into a state space model.

$$\dot{z} = \boldsymbol{A}z + \boldsymbol{B}f_{\boldsymbol{MR}}(t, x_i, \dot{x}_i, v_i) - \boldsymbol{E}\ddot{w}_g \tag{14}$$
$$y = \boldsymbol{C}z + \boldsymbol{D}f_{\boldsymbol{MR}}(t, x_i, \dot{x}_i, v_i) + n$$

where

$$\boldsymbol{A} = \begin{bmatrix} \boldsymbol{O} & \boldsymbol{1} \\ -\boldsymbol{M^{-1}K} & -\boldsymbol{M^{-1}C} \end{bmatrix} \tag{15}$$

$$\boldsymbol{B} = \begin{bmatrix} \boldsymbol{0} \\ \boldsymbol{M^{-1}F} \end{bmatrix} \tag{16}$$

$$\boldsymbol{C} = \begin{bmatrix} \boldsymbol{I} & \boldsymbol{0} \\ \boldsymbol{0} & \boldsymbol{I} \\ -\boldsymbol{M^{-1}K} & -\boldsymbol{M^{-1}C} \end{bmatrix} \tag{17}$$

$$\boldsymbol{D} = \begin{bmatrix} \boldsymbol{0} \\ \boldsymbol{0} \\ \boldsymbol{M^{-1}F} \end{bmatrix} \tag{18}$$

$$\boldsymbol{E} = \begin{bmatrix} \boldsymbol{0} \\ \boldsymbol{F} \end{bmatrix} \tag{19}$$

where $\boldsymbol{F}$ is the location matrix that Chevron braces are located within the building structure, n is the noise vector, and x_i and $\dot{x}_i$ are the displacement and the velocity at the i^{th} floor level of the three-story building structure, respectively. Properties of the three-story building structure are adopted from Dyke et al (1996).

3.1.2. Modeling

In order to present the effectiveness of the WNARMA model for SI, a three-story building employing an MR damper subjected to ambient excitation is considered. The modeling is performed in three different conditions; the structure in a normal condition (Case I), the structure with a time-delayed MR damper forces (Case II), and the structure with stiffness degradation (Case III). Figures 3 to 6 compare the outputs of the NARMA model with the original data with noise of 0%, 10%, 20%, and 30% in Case I. Figure 7 to 10 represent the comparison of the outputs of the WNARMA model with the original data with the noise level of 0%, 10%, 20%, and 30% In Case I. Figure 11 to 14 compare the outputs of the WNARMA model with the original data with noise of 0%, 10%, 20%, and 30% in Case II. Figure 14 to 18 represent the comparison of the outputs of the WNARMA model with the original data with noise level of 0%, 10%, 20%, and 30% in Case III.

Comparing figure 3 to 6 with figure 7 to 10, the outputs of the WNARMA model contains less high frequency noise components than those of the outputs using the NARMA model. It is because the WNARMA model employs the WT, which filters out high frequency

noise components of the signal. As shown in figure 7 to 10, the high frequency rejection characteristics get clearer as the percentage of the noise increases. In addition, as shown in figure 3 to 10, the time length of the outputs of the NARMA model is 500 seconds while the time length of the outputs of the WARMA model is 15 seconds. The time length of the outputs of the WNARMA model is about 33 times shorter than those of the outputs of the NARMA model, which allows significant reduction of the computation time. Therefore, it can be summarized that the WNARMA model is more time efficient than NARMA model when modeling the vibration signals from the smart structure.

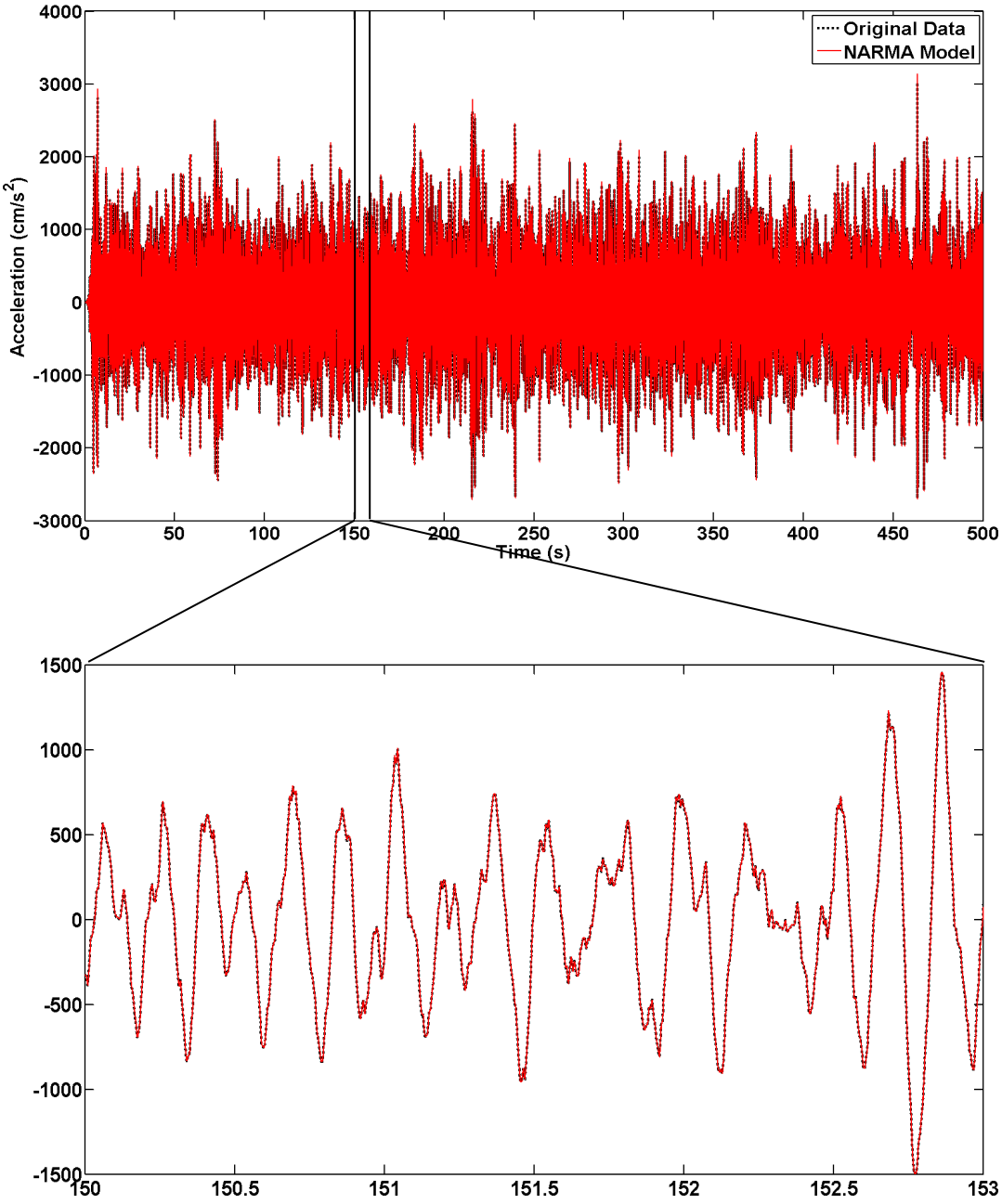

Figure 3. Comparison of the NARMA with the origianl data with free noise (Case I)

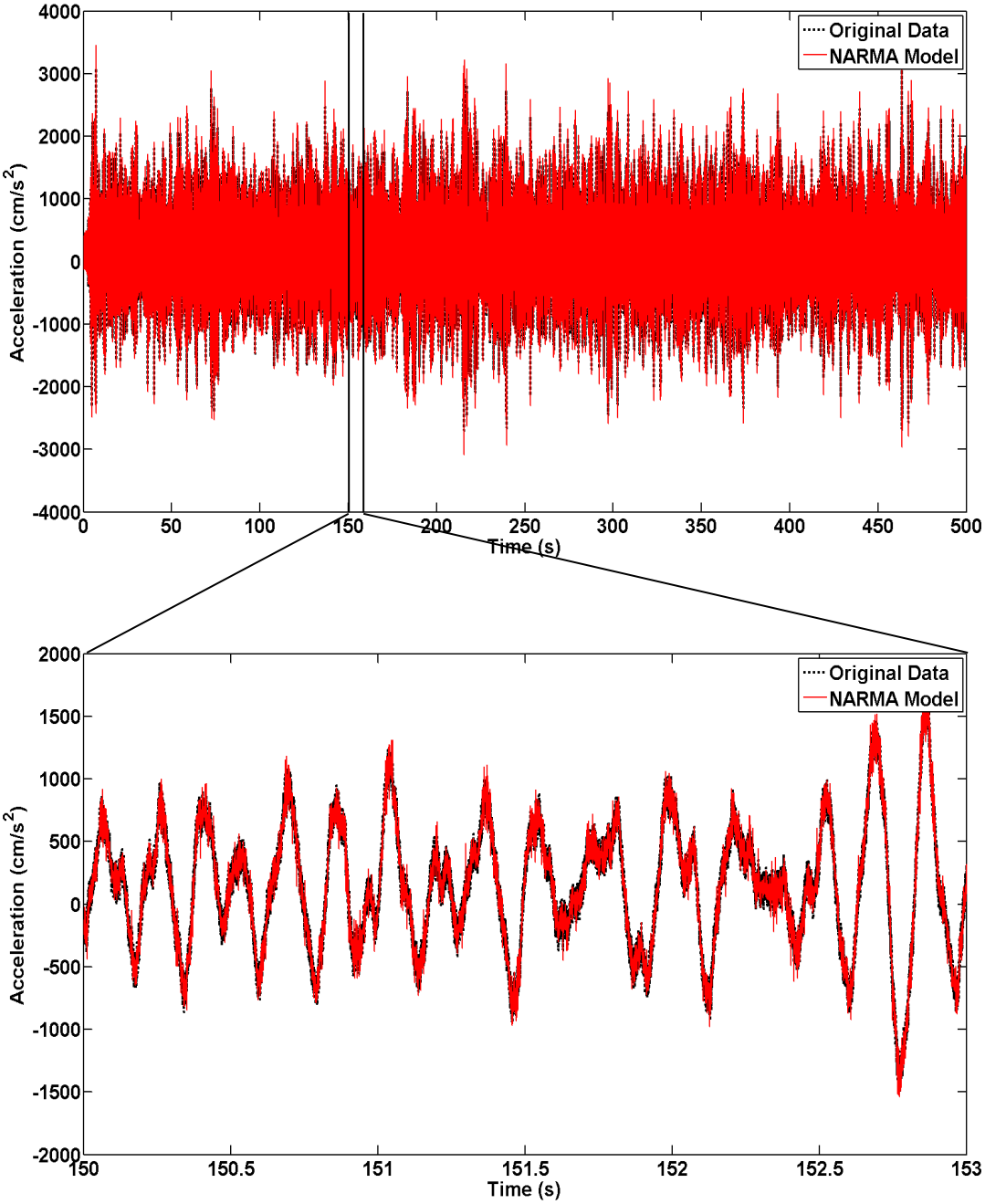

Figure 4. Comparison of the NARMA with the origianl data with 10% noise (Case I)

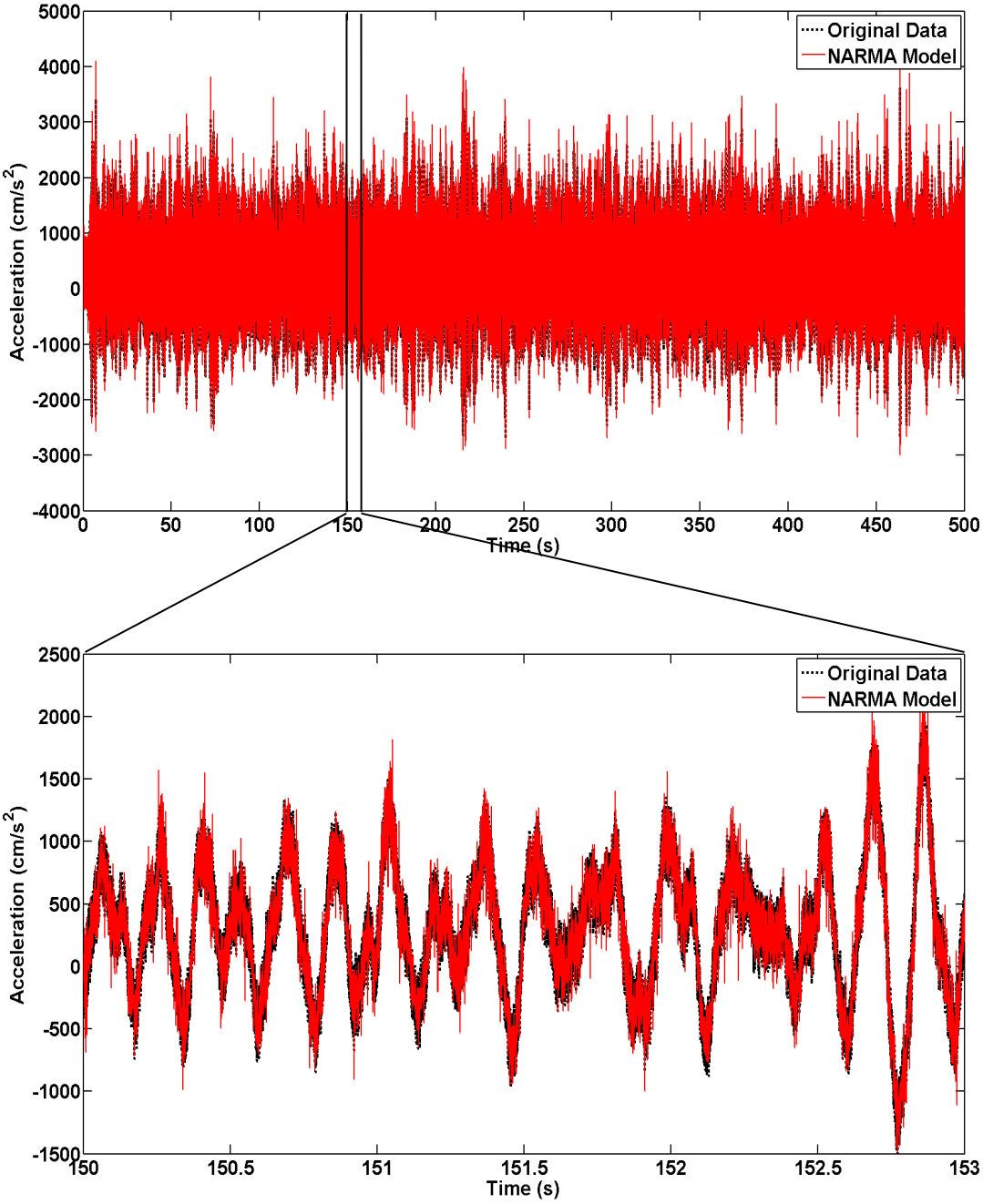

Figure 5. Comparison of the NARMA with the origianl data with 20% noise (Case I)

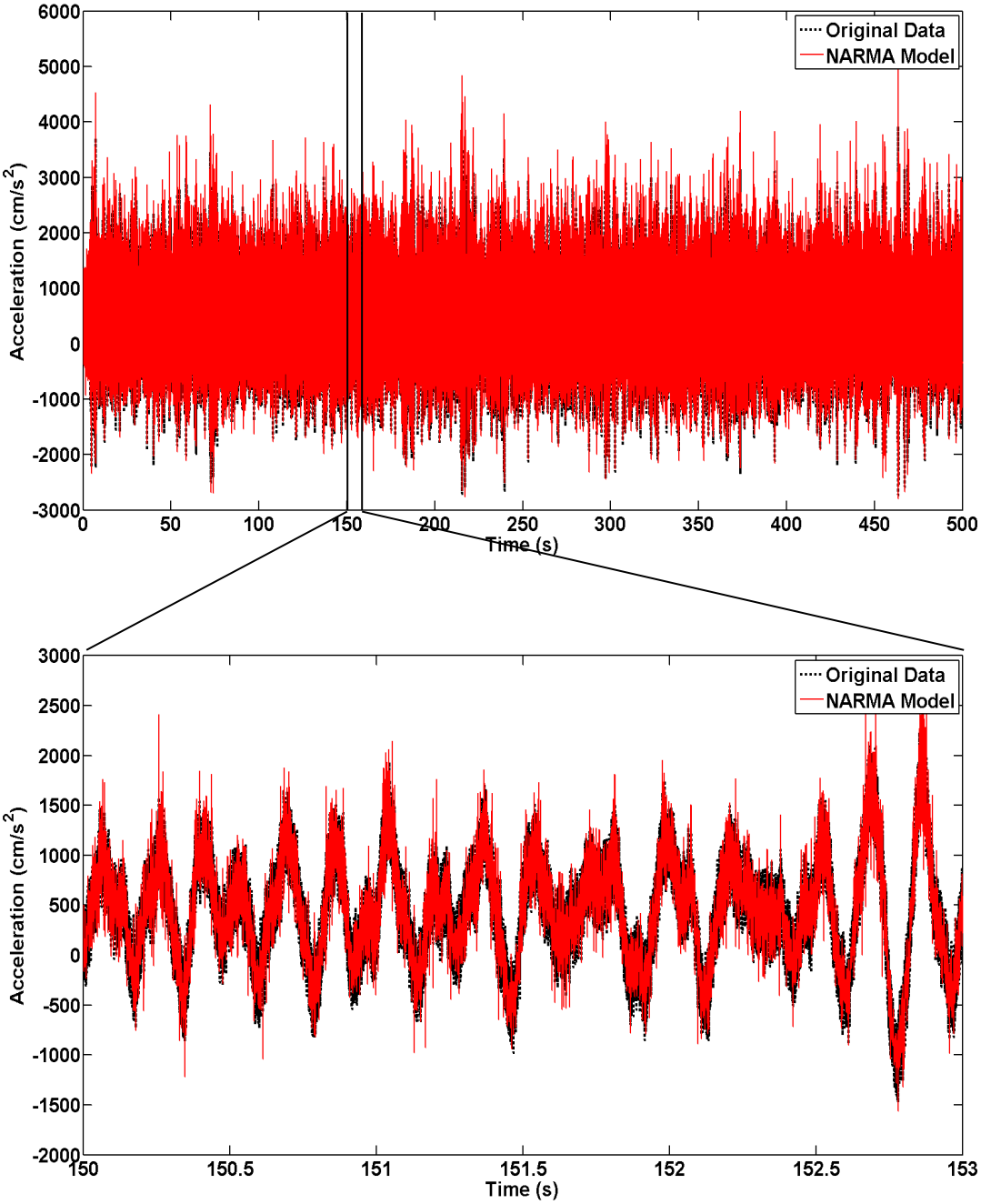

Figure 6. Comparison of the NARMA with the original data with 30% noise (Case I)

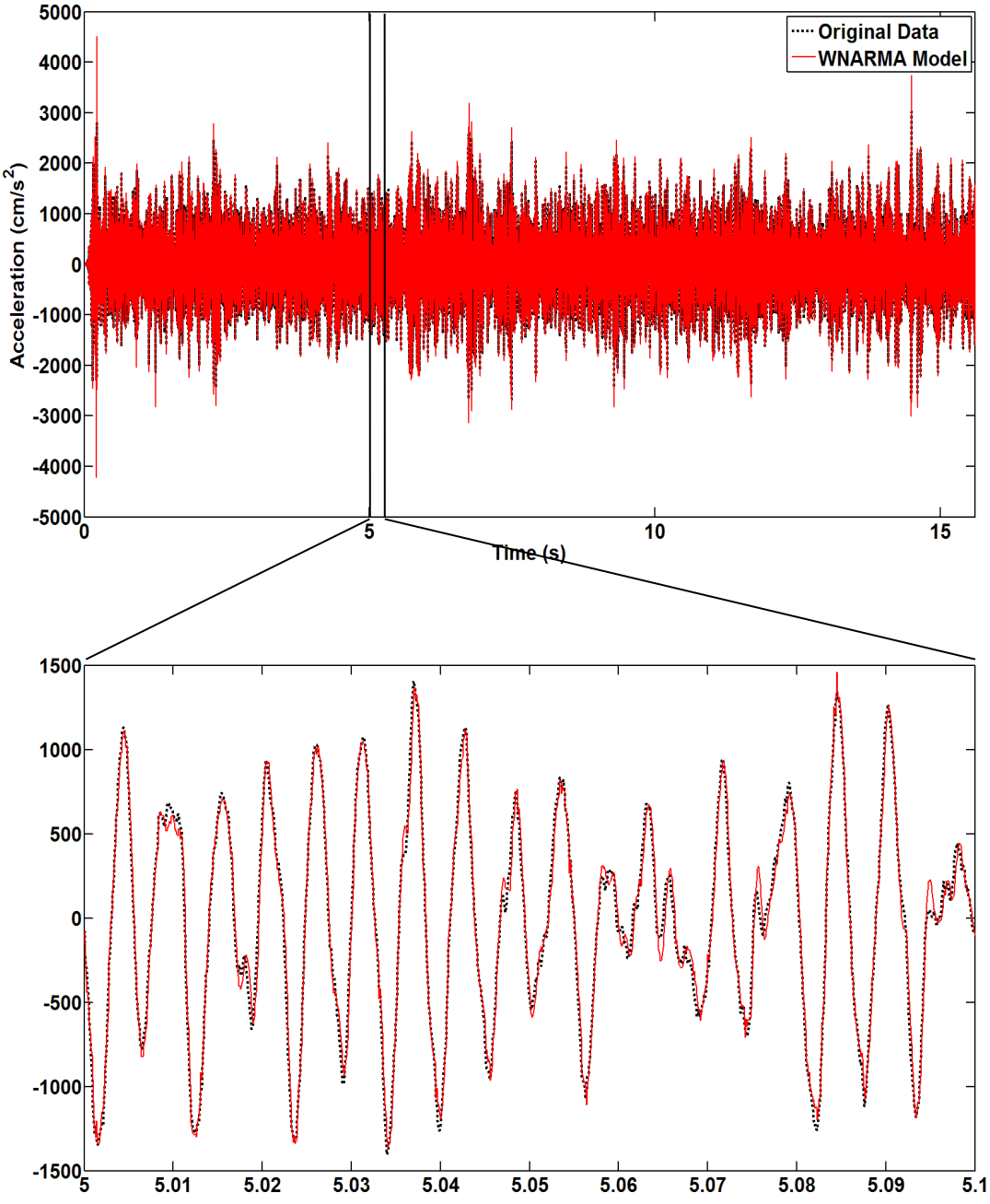

Figure 7. Comparison of the WNARMA with the original data with noise free (Case I)

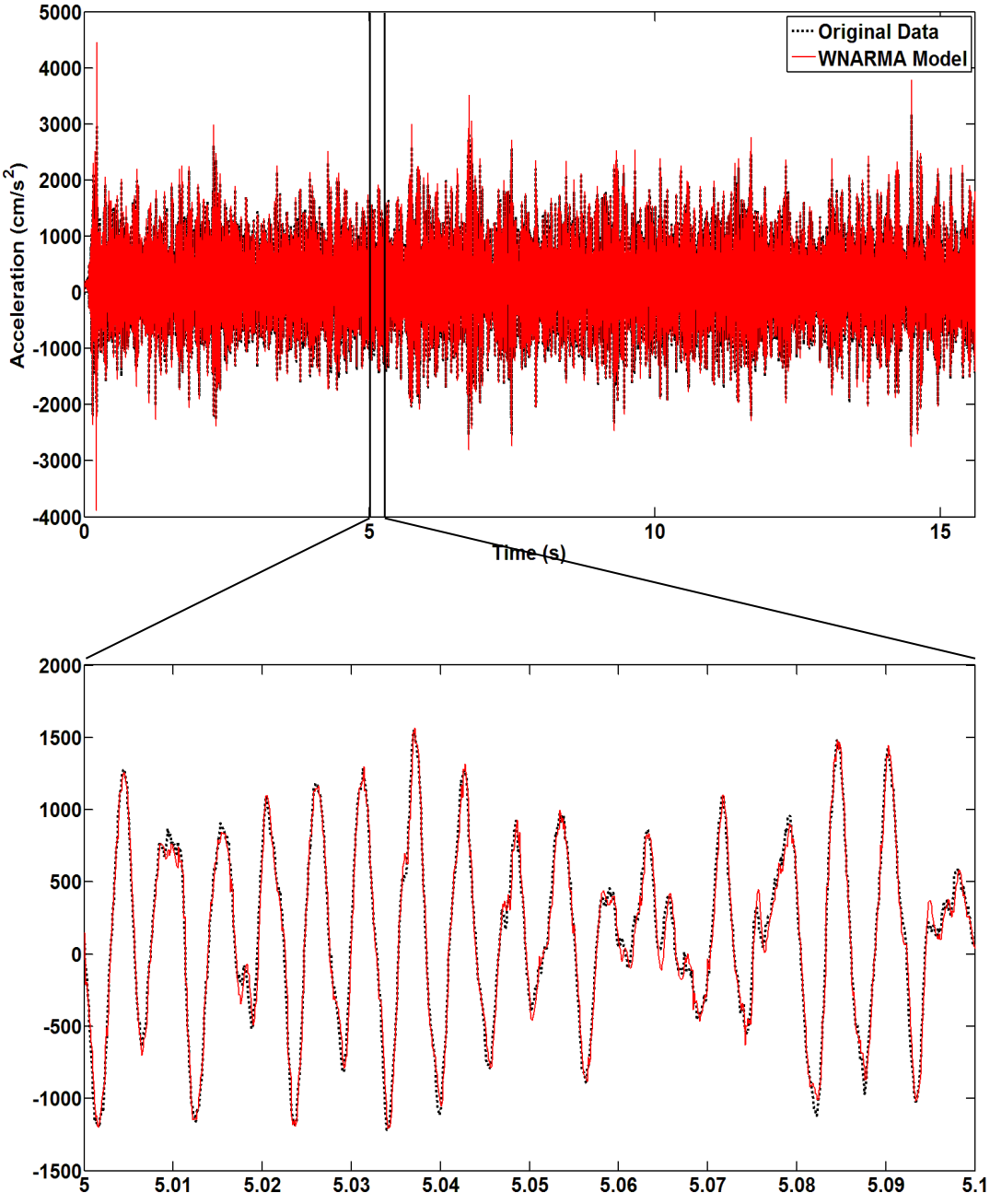

Figure 8. Comparison of the WNARMA with the origianl data with 10% noise (Case I)

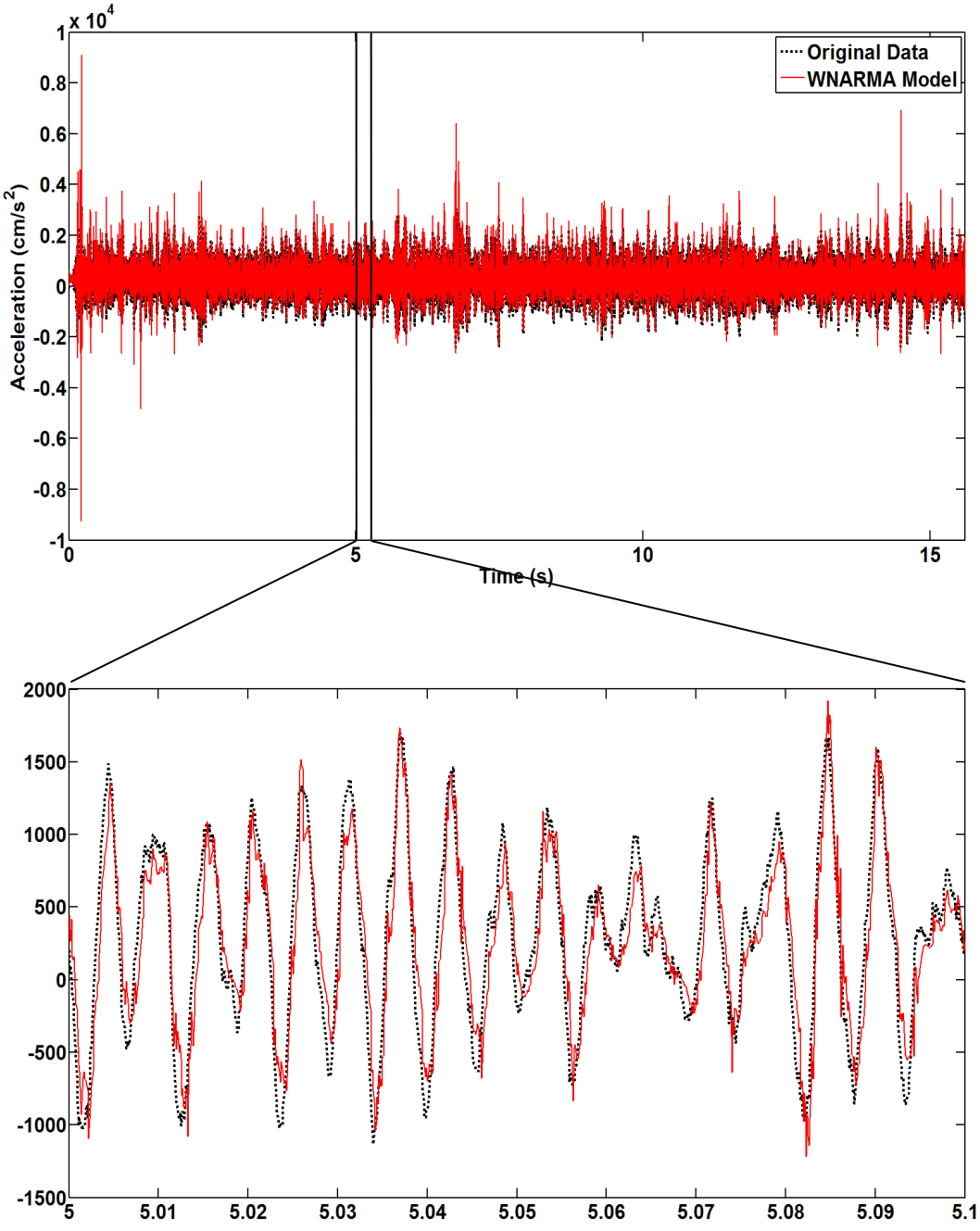

Figure 9. Comparison of the WNARMA with the original data with 20% noise (Case I)

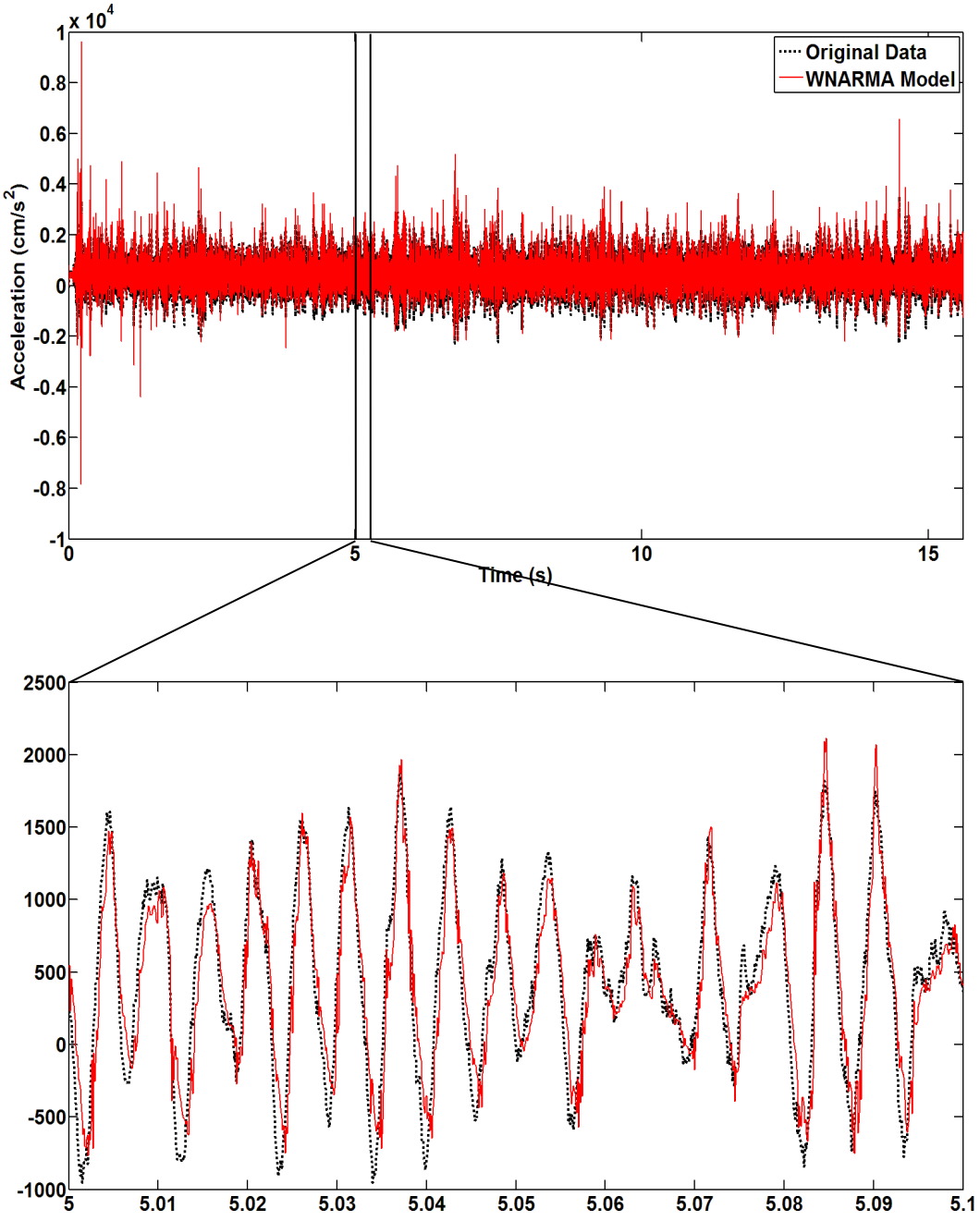

Figure 10. Comparison of the WNARMA with the original data with 30% noise (Case I)

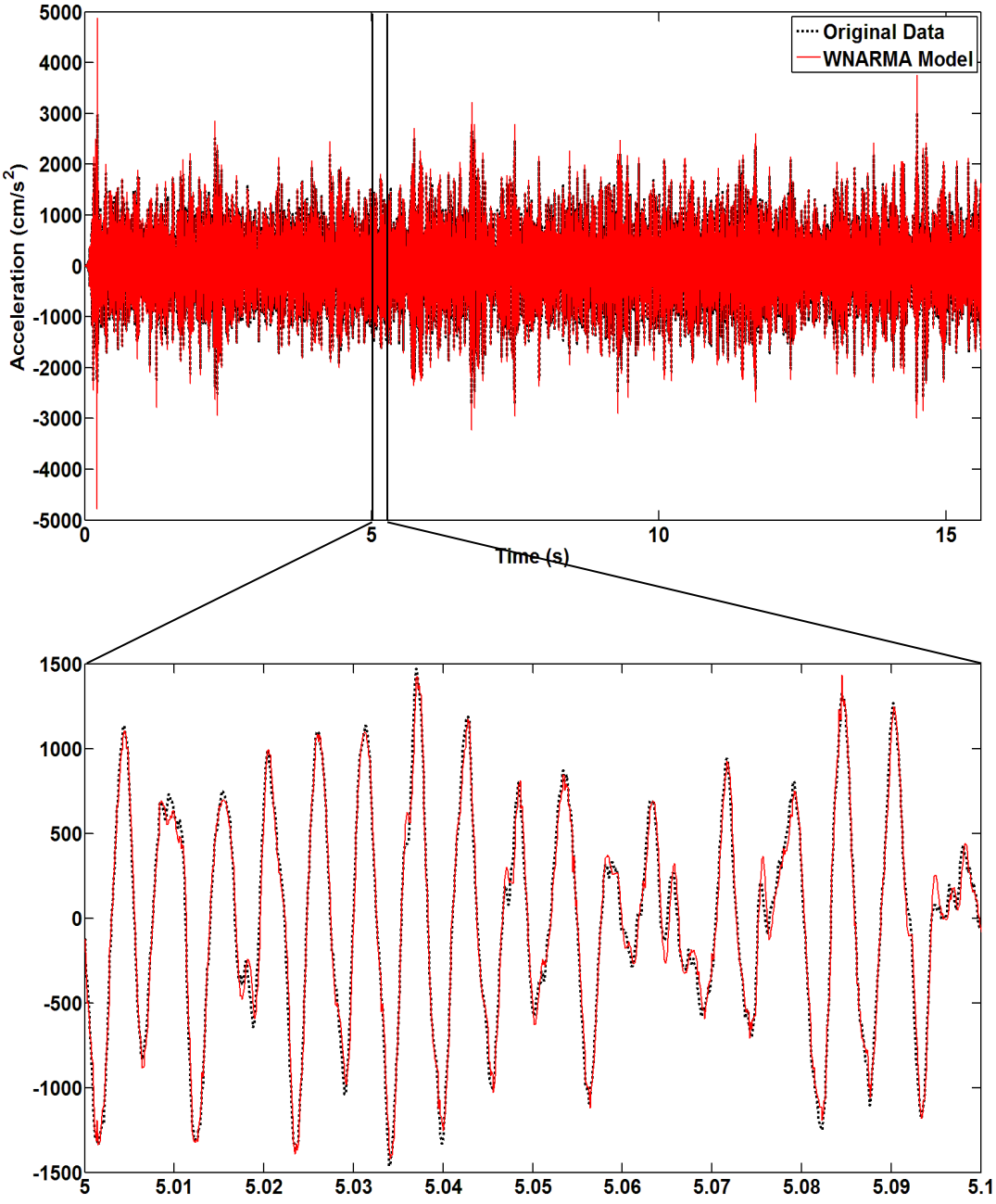

Figure 11. Comparison of the WNARMA with the original data with noise free (Case 2)

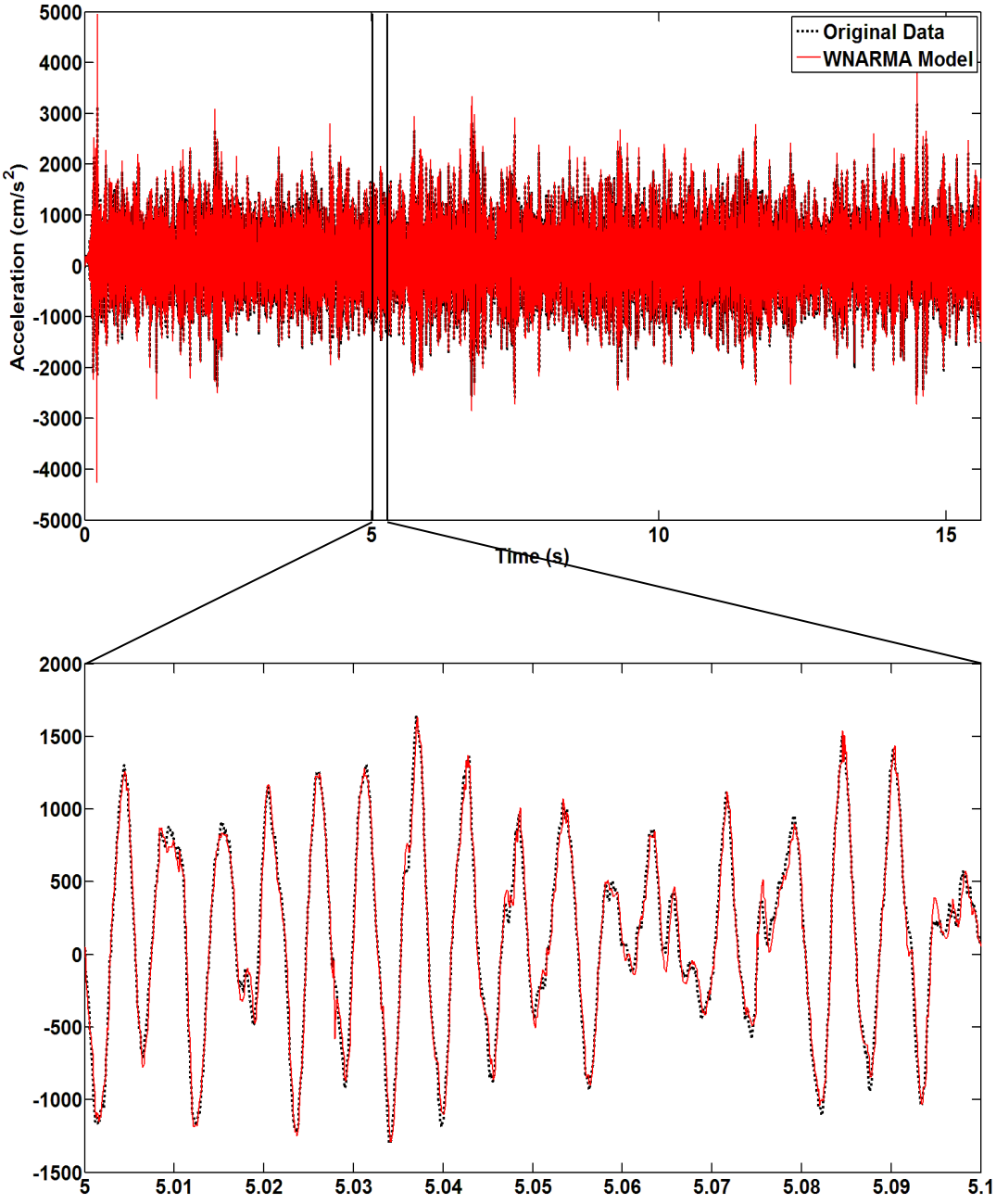

Figure 12. Comparison of the WNARMA with the original data with 10% noise (Case II)

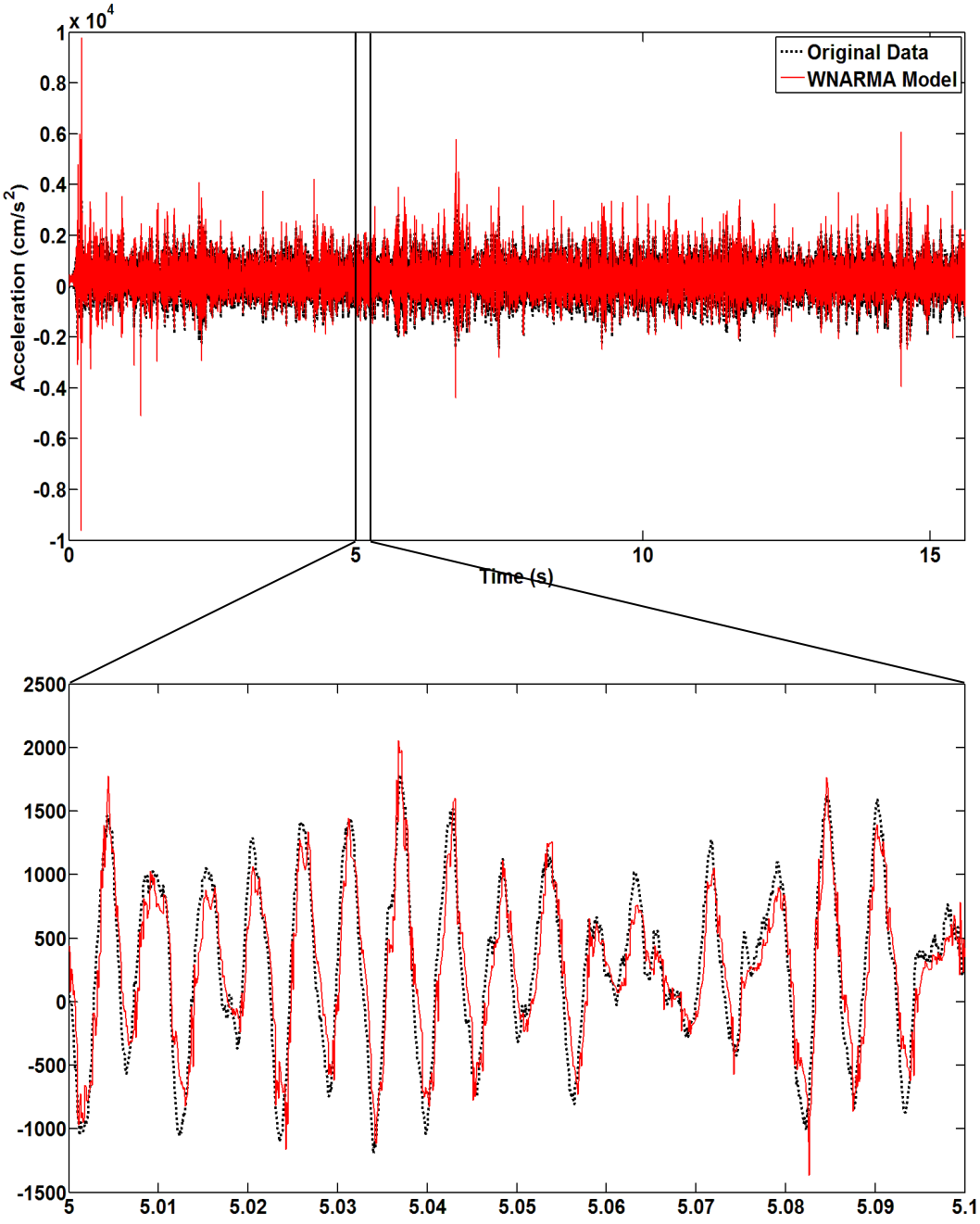

Figure 13. Comparison of the WNARMA with the original data with 20% noise (Case II)

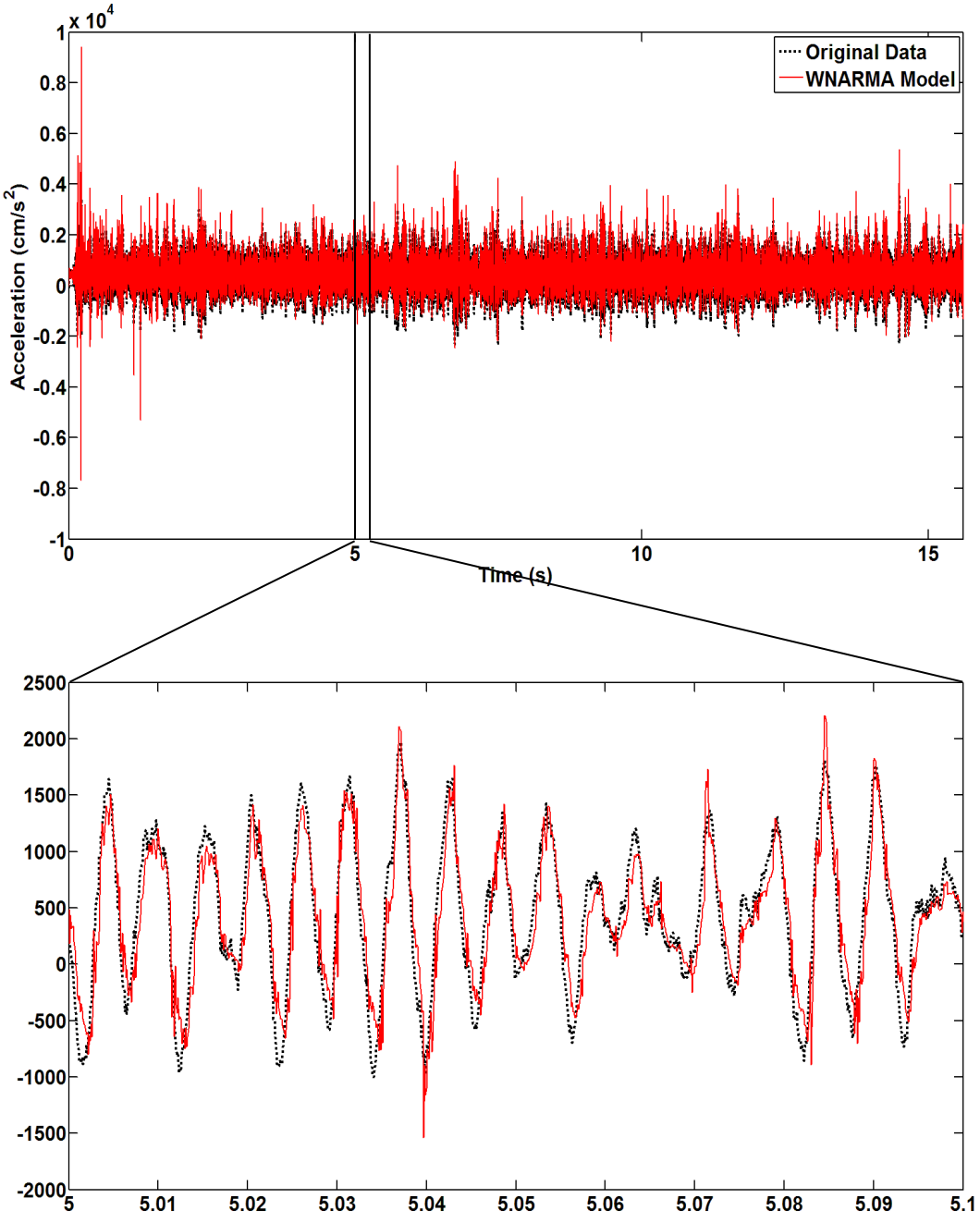

Figure 14. Comparison of the WNARMA with the original data with 30% noise (Case II)

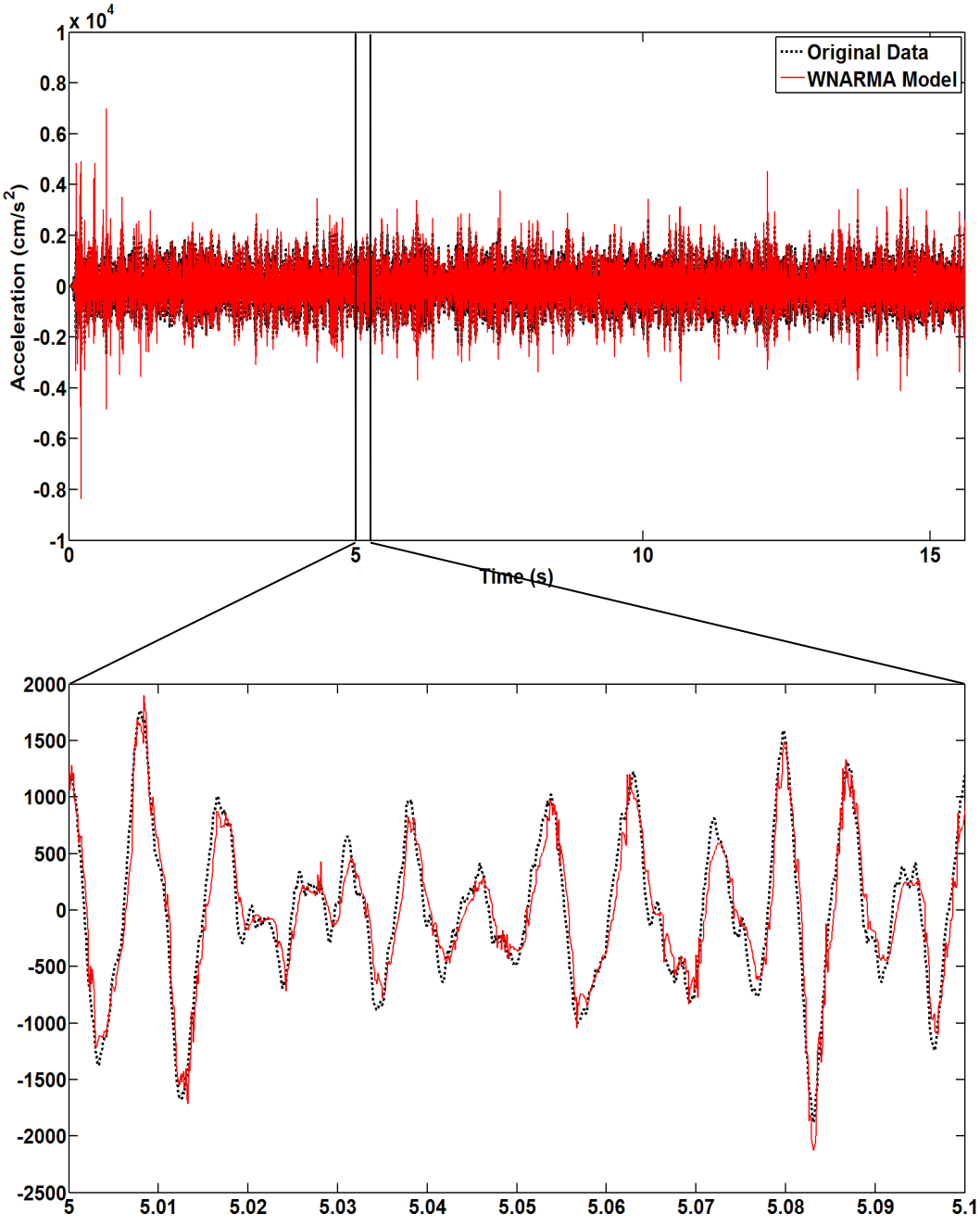

Figure 15. Comparison of the WNARMA with the origial data with noise free (Case III)

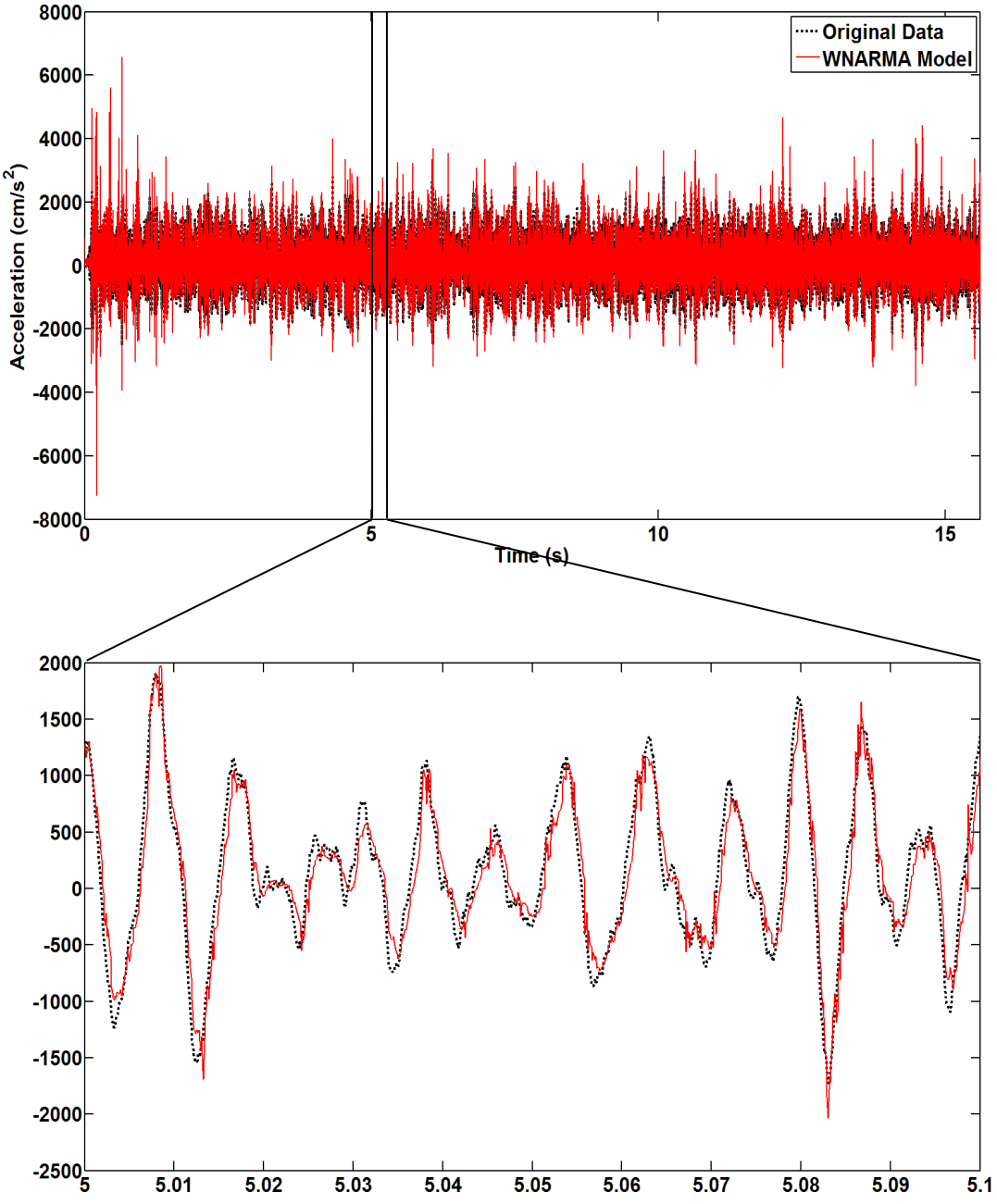

Figure 16. Comparison of the WNARMA with the original data with 10% noise (Case III)

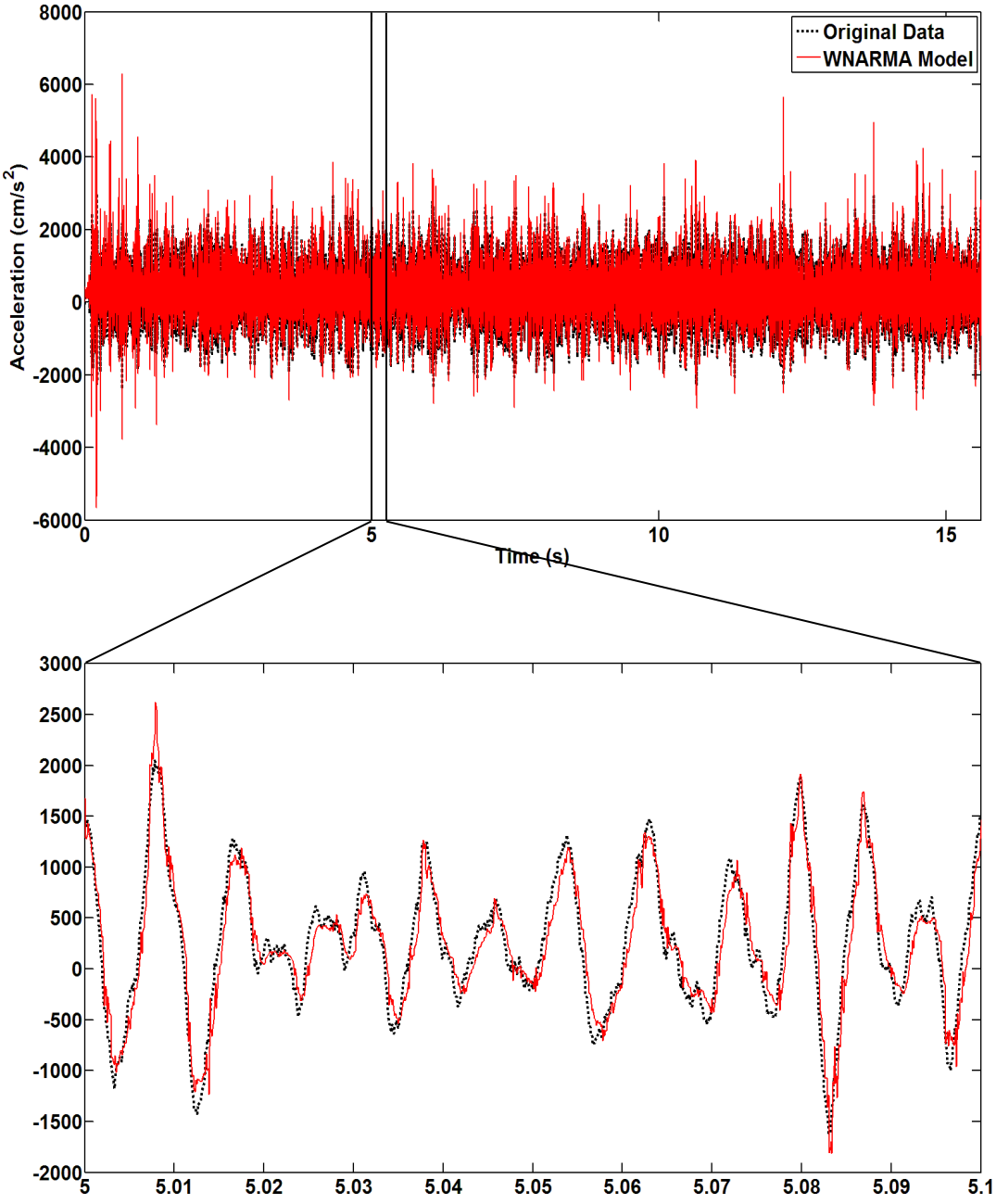

Figure 17. Comparison of the WNARMA with the original data with 20% noise (Case III)

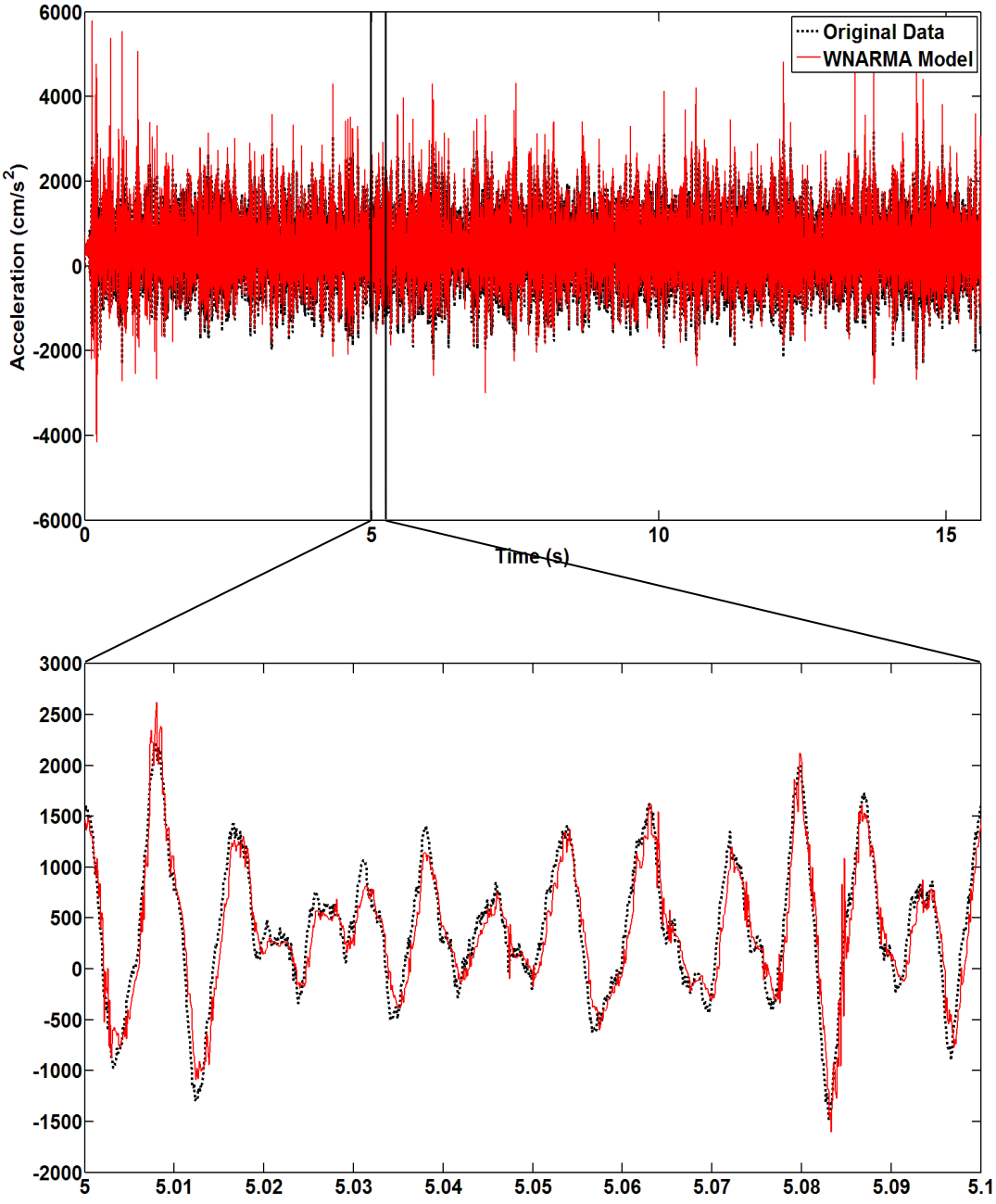

Figure 18. Comparison of the WNARMA with the origianl data with 30% noise (Case III)

In order to examine the performance of the proposed model, it can be compared to the original response of the structure. Table 1 compares the performance of the NARMA and WNARMA models. The first evaluation index, J_1, is

$$J_1 = max|\hat{y} - \tilde{y}| \tag{20}$$

where $\hat{y}$ is the estimation, $\tilde{y}$ is the actual structural response data. The second evaluation index, J_2, is

$$J_2 = min|\hat{y} - \tilde{y}| \tag{21}$$

As the third evaluation index, J_3, the root mean square error (RMSE) is considered and given by

$$J_3 = RMSE = \sqrt{\frac{\sum(|\hat{y} - \tilde{y}|)^2}{N}} \tag{22}$$

where N is the number of data points. As the forth evaluation index, J_4, the fitting rate (FR) is obtained by

$$J_4 = FR = \left[1 - \frac{|\tilde{y} - \hat{y}|}{|\tilde{y} - \bar{y}|}\right] \times 100 \tag{23}$$

where $\bar{y}$ is the mean value of the actual structural response data. If the proposed model produces the same responses as the data, FR is 100. The last evaluation index, J_5, is the computational load given by

$$J_5 = CPU\ time \tag{24}$$

Table 1. Training Results for NARMA and WNARMA Models

		Noise-free		Noise (10%)		Noise (20%)		Noise (30%)	
		NARMA	WNARMA	NARMA	WNARMA	NARMA	WNARMA	NARMA	WNARMA
Case I	J1	235.90	2860.2	530.11	2688.6	1179.9	7793.7	1461.1	6529.3
	J2	8.75E-07	2.29E-06	2.77E-05	5.08E-05	1.63E-05	4.25E-05	8.28E-05	5.21E-05
	J3	11.91	86.98	52.98	91.91	103.44	241.69	152.99	246.26
	J4	99.96	97.92	99.25	98.00	97.33	85.85	94.69	86.59
	J5	1414.73	40.21	1449.64	38.78	1522.43	42.43	1398.72	41.01
Case II	J1	236.62	3351.2	609.63	2759.0	1001.4	7813.7	1647.7	6354.5
	J2	1.65E-06	1.07E-06	1.44E-05	4.08E-05	8.20E-04	3.73E-05	4.03E-04	5.14E-05
	J3	11.49	89.64	53.74	94.51	103.46	245.14	151.39	249.20
	J4	99.93	97.86	98.88	97.91	96.22	85.77	92.85	86.52
	J5	1452.24	41.24	1423.46	43.83	1363.22	44.24	1381.27	40.35
Case III	J1	325.30	6721.2	377.02	6199.7	674.62	5864.6	1111.8	4848.9
	J2	3.44E-08	4.39E-07	9.64E-05	1.57E-05	1.81E-04	3.10E-05	2.67E-05	4.31E-05
	J3	13.18	215.23	48.88	218.47	94.14	225.99	138.42	233.13
	J4	99.96	90.72	99.27	90.72	97.47	90.54	94.99	90.85
	J5	1477.19	45.45	1422.86	46.42	1504.32	47.84	1562.51	45.71

As shown in table 1, the overall training time of the WNARMA model is about 35 times faster than that of the NARMA without significantly degrading the modeling accuracy. The fitting rate of the WANAMA is over 85% for all the cases. In other words, even with a drastic reduction in

computational loads, the WNARMA models provide good fitting rates. It also provides a noise reduction scheme.

3.1.3.Conclusion

In this paper, a novel time series model is proposed for system identification (SI) of smart structures subjected to ambient excitation. The new model is developed through the integration of wavelet transform (WT) and nonlinear autoregressive moving average (ARMA) models. To evaluate the performance of the proposed approach, a three-story building equipped with a magnetorheological (MR) damper is studied. It is demonstrated from the simulation that the proposed model is effective in predicting the nonlinear behavior of smart structures under ambient excitations. Since the WNARMA model compresses the data obtained from the smart structure, it is able to reduce the computation time significantly. The overall training time of the WNARMA model is about 35 times less than that of the nonlinear ARMA (NARMA) model with the 2% deviation of fitting rate. In addition, the proposed model is robust against a variety of noise levels.

3.2. Case study 2

As the dynamic response and energy absorbing characteristics of a structure under impact loads can be cost-effectively analyzed using drop tower test equipment, the proposed experimental system is comprised of a drop tower test equipment, a reinforced concrete beam, an MR damper, sensors, a high speed camera, and a data acquisition system. A concrete structure employing an MR damper is impacted by a pre-determined falling mass using the drop-tower test equipment; the dynamic response and energy absorbing characteristics of the structure are monitored and

captured by the sensors and a high-speed camera, and the recorded data is analyzed from the data acquisition system.

3.2.1. Experimental setup

A drop tower test is conducted in Structural Mechanics and Impact Laboratory in the Civil and Environmental Engineering Department at Worcester Polytechnic Institute using the drop tower test equipment, which shown in figure 19. The drop tower test equipment with a capacity of 22,500 kg is used for this test. For the test specimen, a simply supported reinforced concrete beam with a size of 10x10x100 cm is used, which is shown in figure 20. The steel reinforcement includes 6 longitudinal reinforcing bars, which has a diameter of 0.75 cm with a tensile yield strength of 248 MPa, and the diameters of steel wires of 0.25 cm with a spacing of 7.5 cm are used for stirrups. The concrete beam, which is made of Portland cement with aggregate size of 6.5 mm, is used after curing for over three weeks. The compressive strength and modulus of elasticity of the concrete are 26 MPa and 15 GPa. The configuration of steel reinforcement is depicted in figure 21.

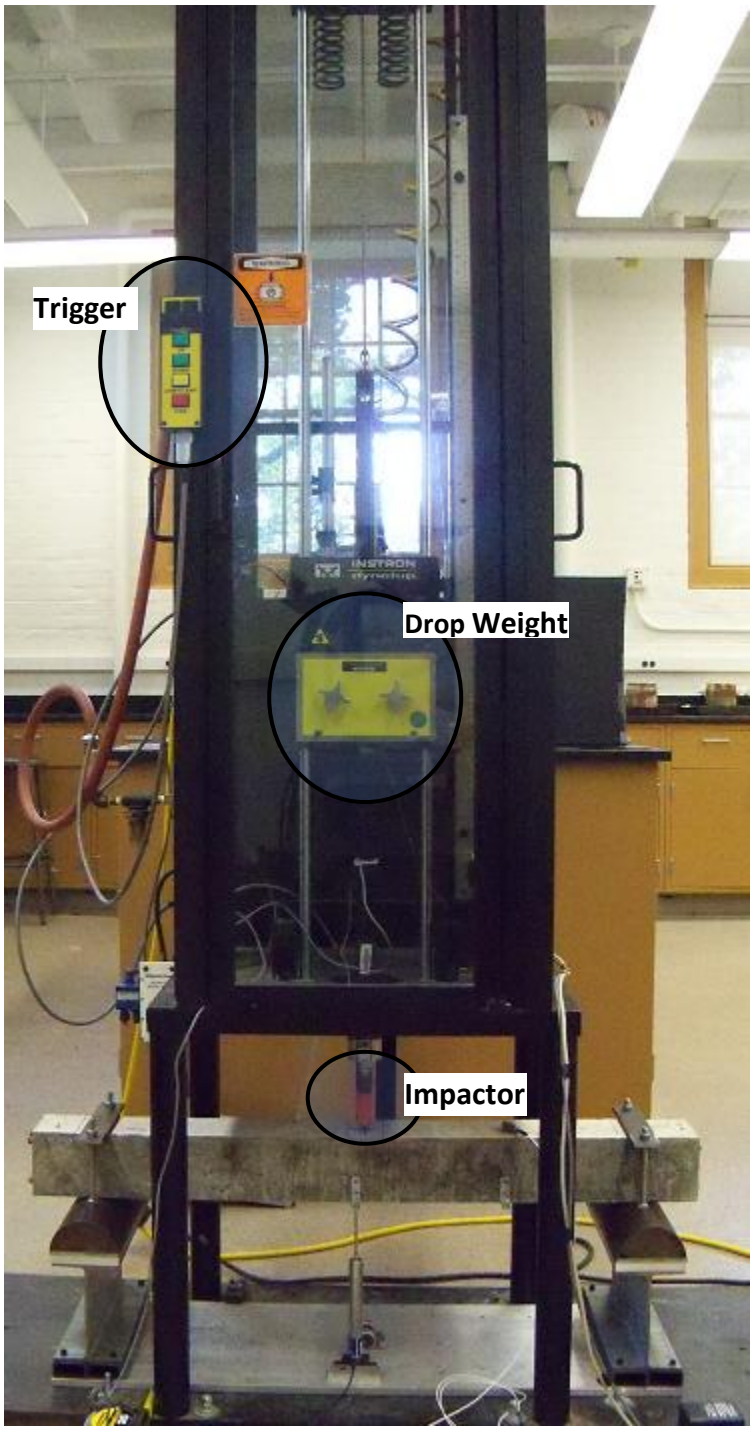

Figure 19. Drop-tower test equipment with a capacity of 22,500 kg

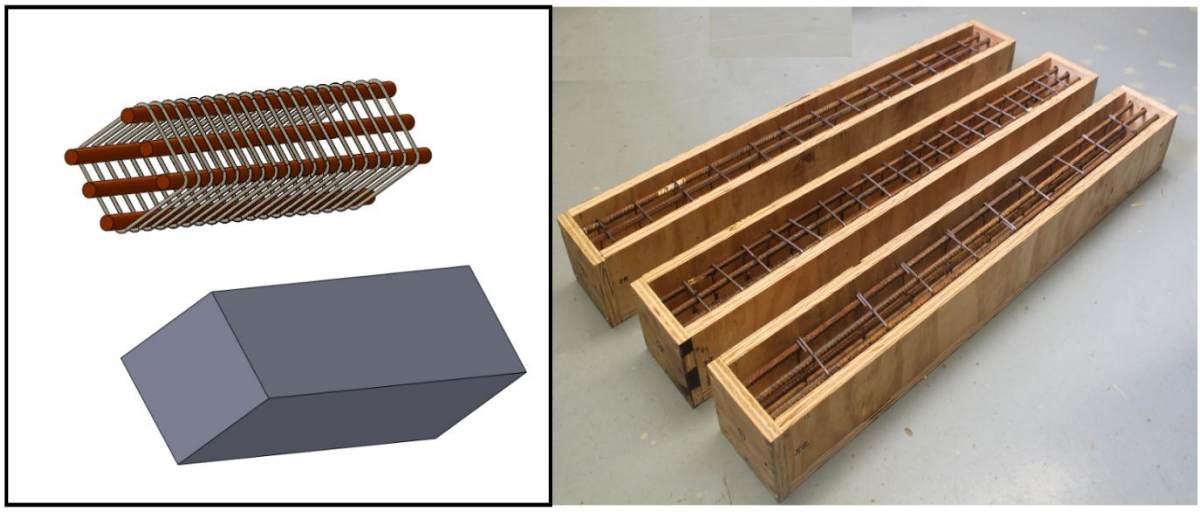

Figure 20. Prepared concrete beams

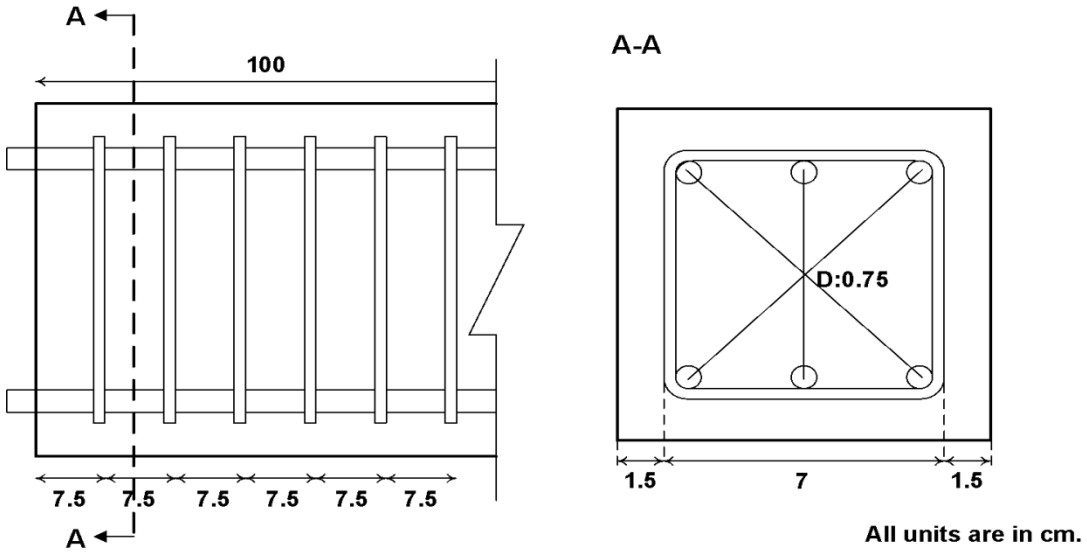

Figure 21. Configuration of reinforcement

An MR damper, which is shown in Figure 22, is installed beneath the mid-span of the reinforced concrete beam to mitigate the impact from the falling mass.

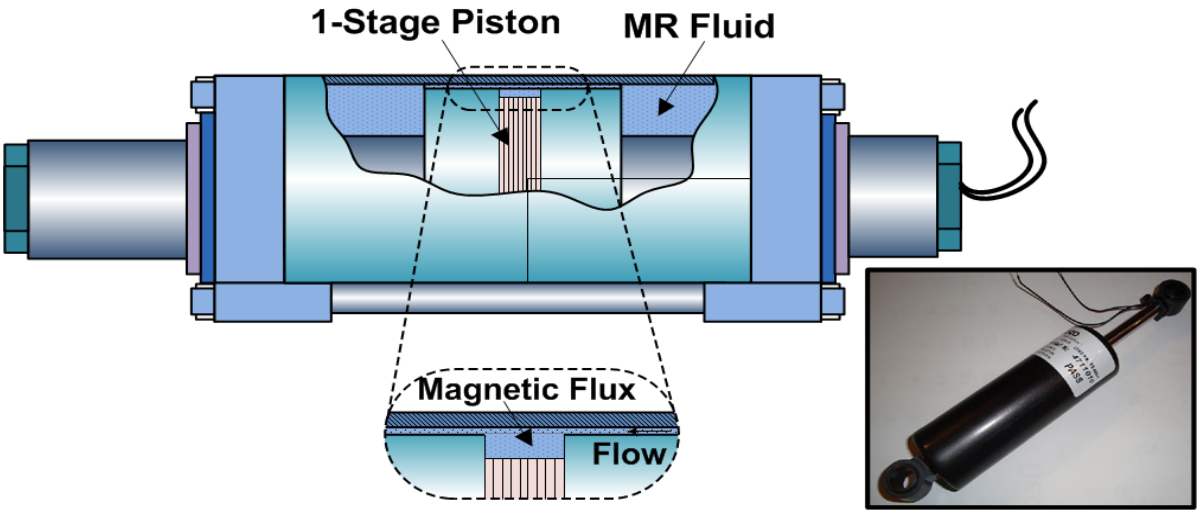

Figure 22. Magnetorheological (MR) damper

3.2.2. Data acquisition

In order to collect data such as acceleration, deflection, strain, and impact force, National Instrument (NI) labview data acquisition system is used with five sensors in the impact test; the acceleration is measured using two accelerometers (PCB 302A); the deflection is measured from one ACT LVDT displacement transducer (RDP Electronics), which is placed at the middle of the beam; the strain is measured from one M.M product N2A series strain gauge; the applied impact force is measured using 4,500 kg capacity Central HTC-10K type load cell; the data acquisition system samples 10,000 data points per second. Figure 23 shows how these sensors are placed.

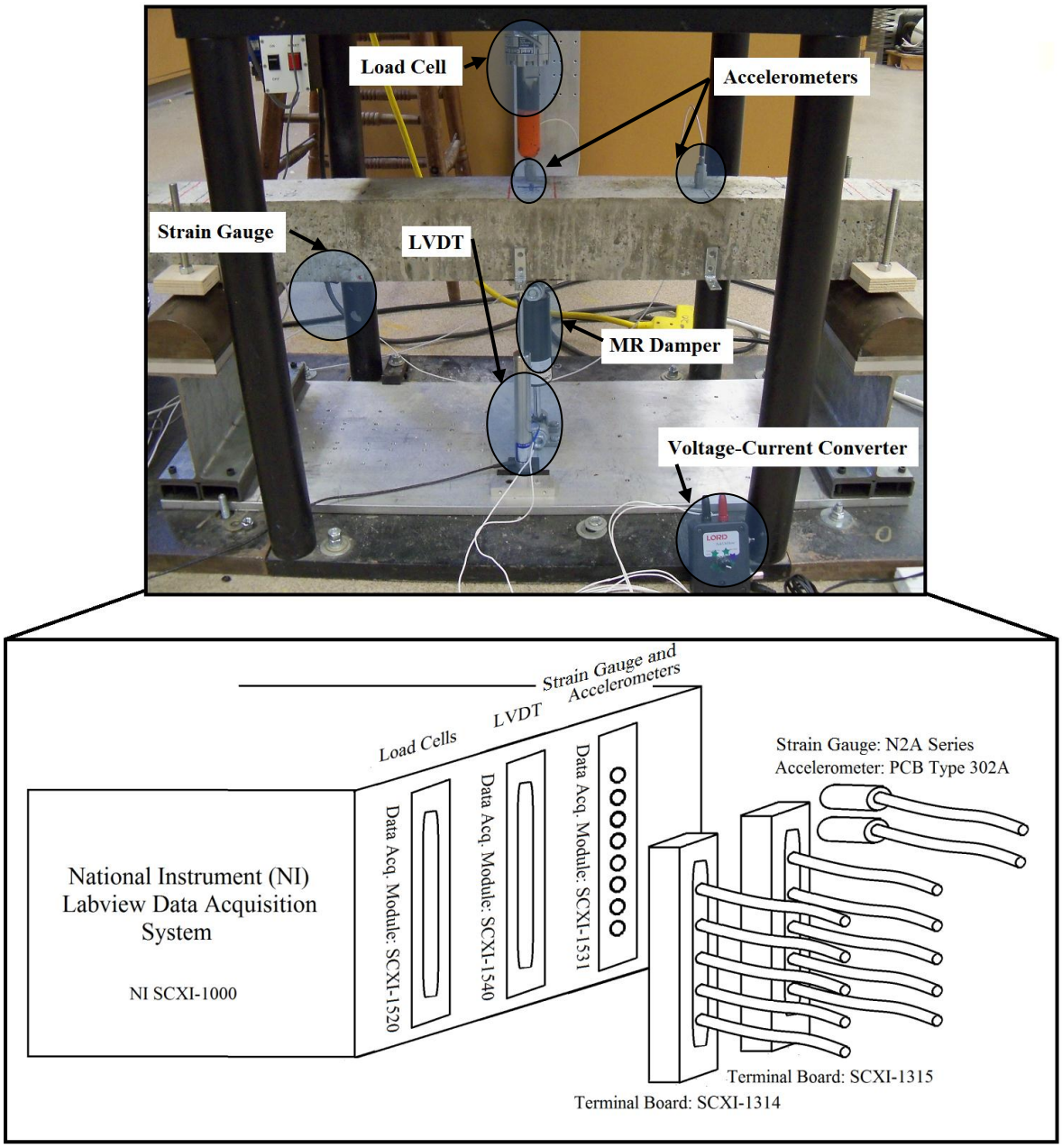

Figure 23. Configuration of the sensors and data acquisition system

3.2.3. Modeling

In order to show the effectiveness of the WNARMA model for SI, a reinforced concrete structure employing an MR damper subjected to a high impact load is considered. The WNARMA modeling is performed in six different conditions when the tested structure is undamaged (healthy) and damaged (5%, 10%, 15%, 30%, and 50%, respectively). The characteristics of the tested structure are changed by adding different masses to the undamaged structure. For each condition, acceleration, deflection and strain are measured from 100 times of impact tests. Figures 24 to 31 show the outputs of modeling using NARMA model when the tested structure is not damaged. Figure 24 to 27 show the outputs of modeling in the best cases while figure 29 to 31 show the outputs of modeling in the worst cases. Figure 32 to 39 show the outputs of modeling using WNARMA model when the tested structure is not damaged. Figure 32 to 35 show the outputs of modeling in the best cases while figure 36 to 39 show the outputs of modeling in the worst cases.

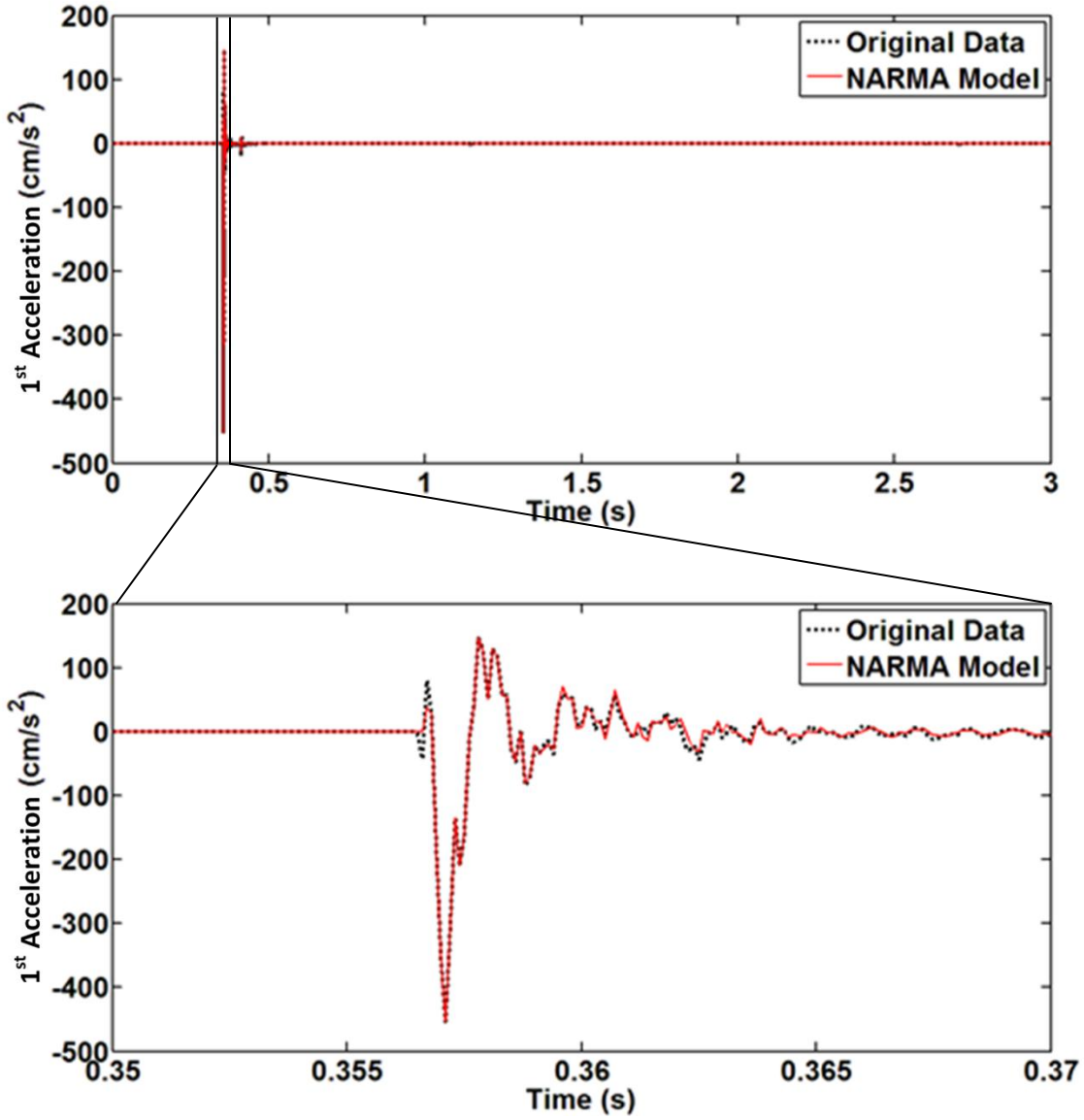

Figure 24. Comparison of the NARMA with the original data (best case)

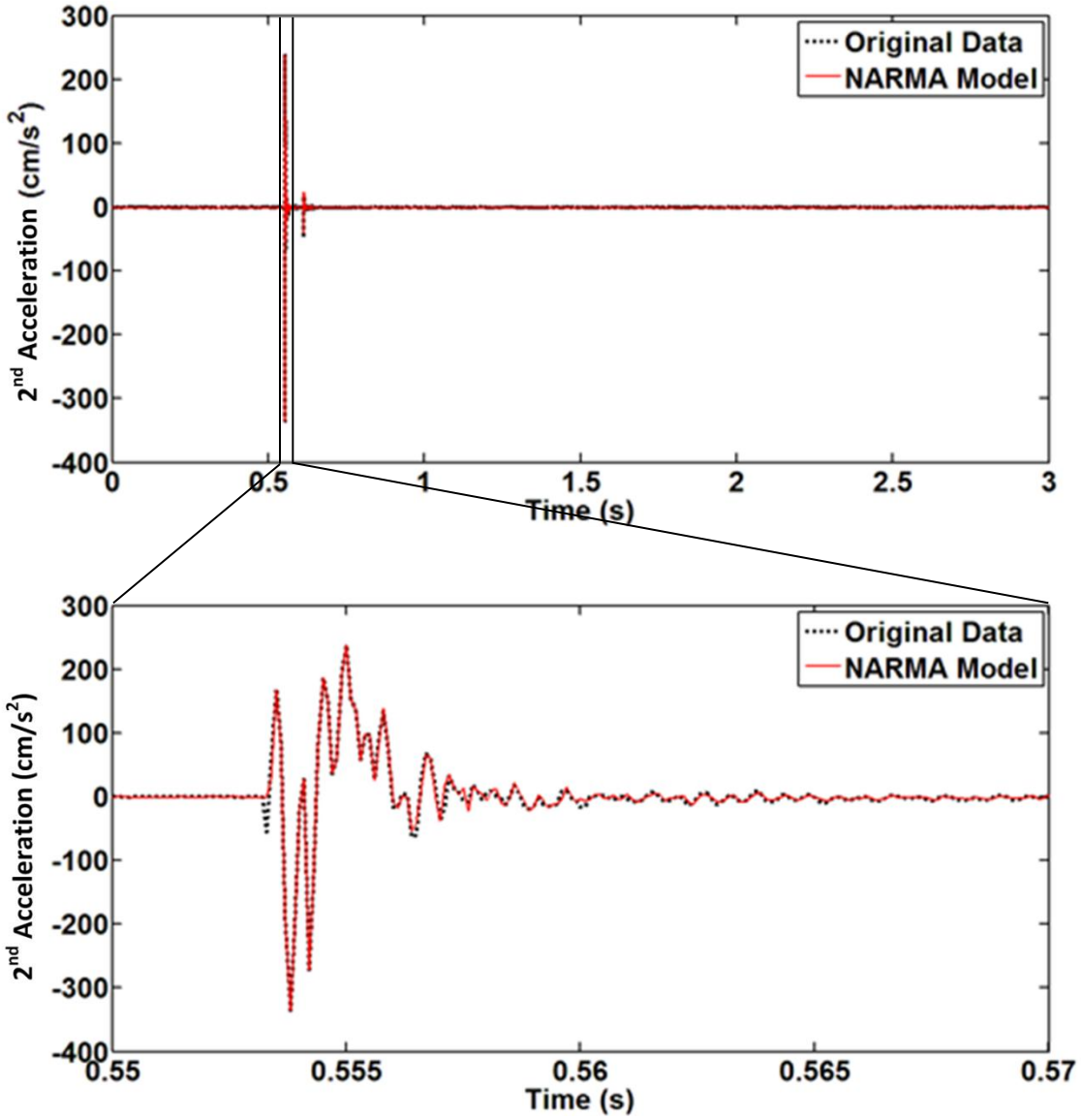

Figure 25. Comparison of the NARMA with the original data (best case)

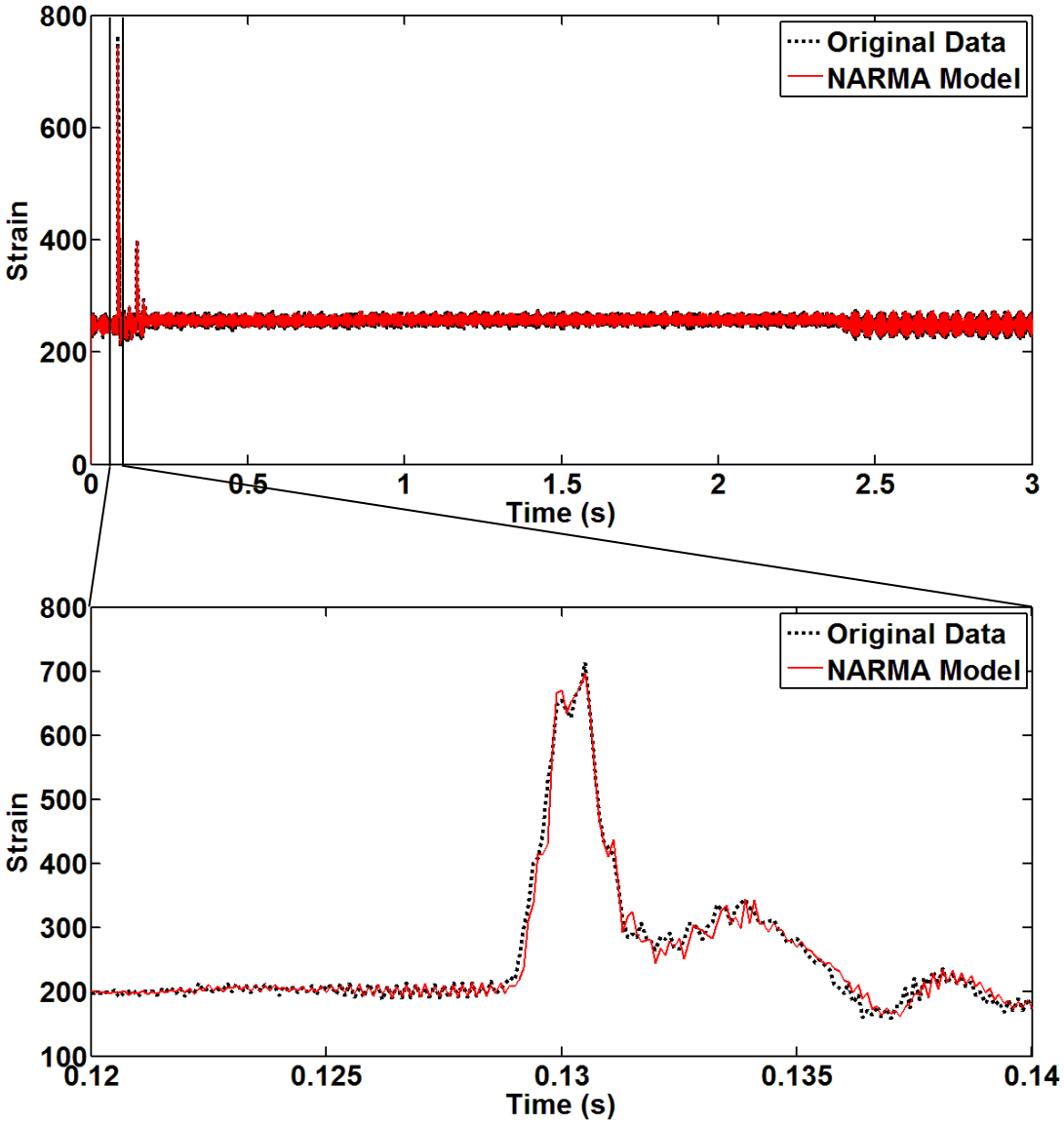

Figure 26. Comparison of the NARMA with the original data (best case)

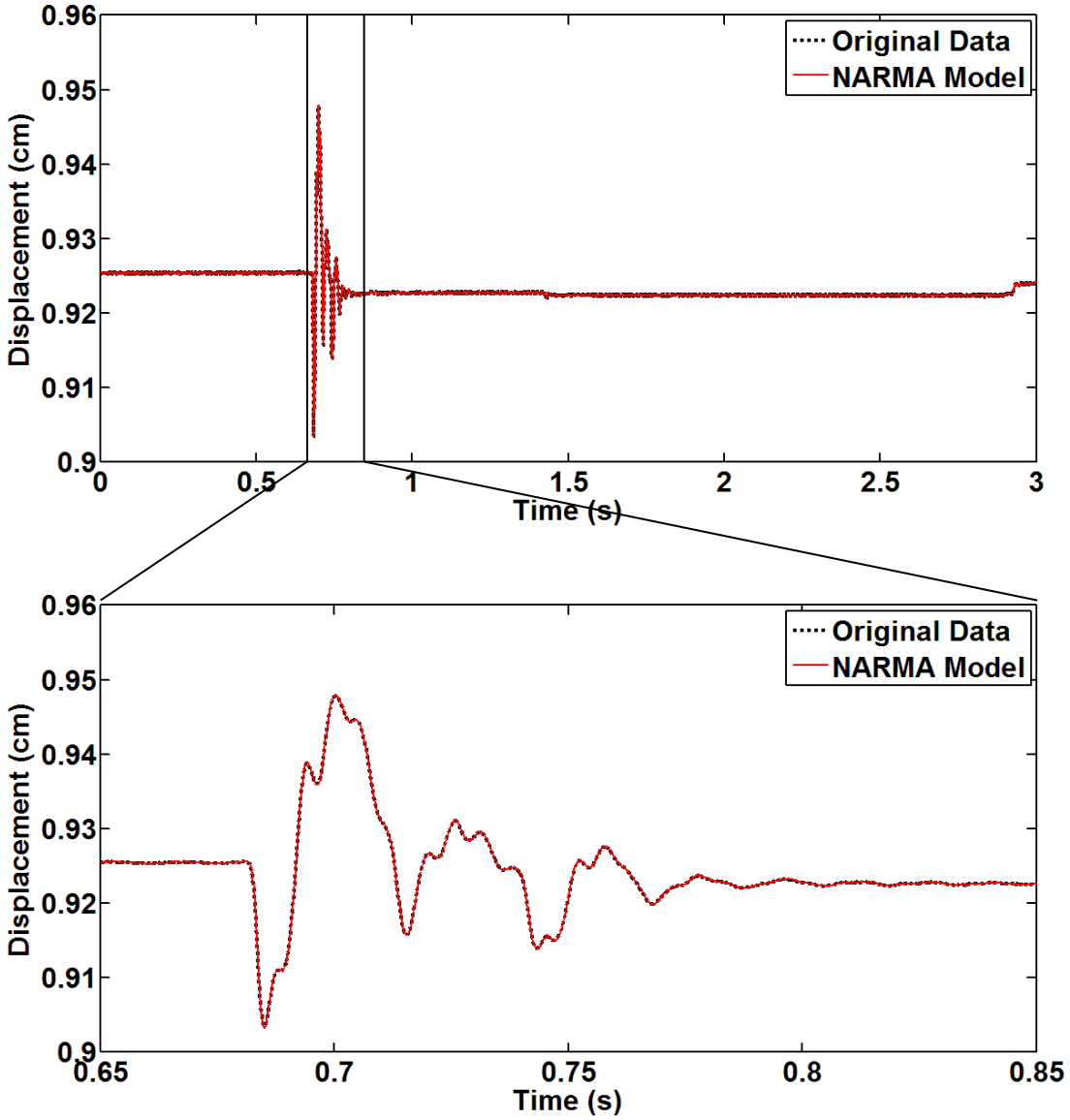

Figure 27. Comparison of the NARMA with the original data (best case)

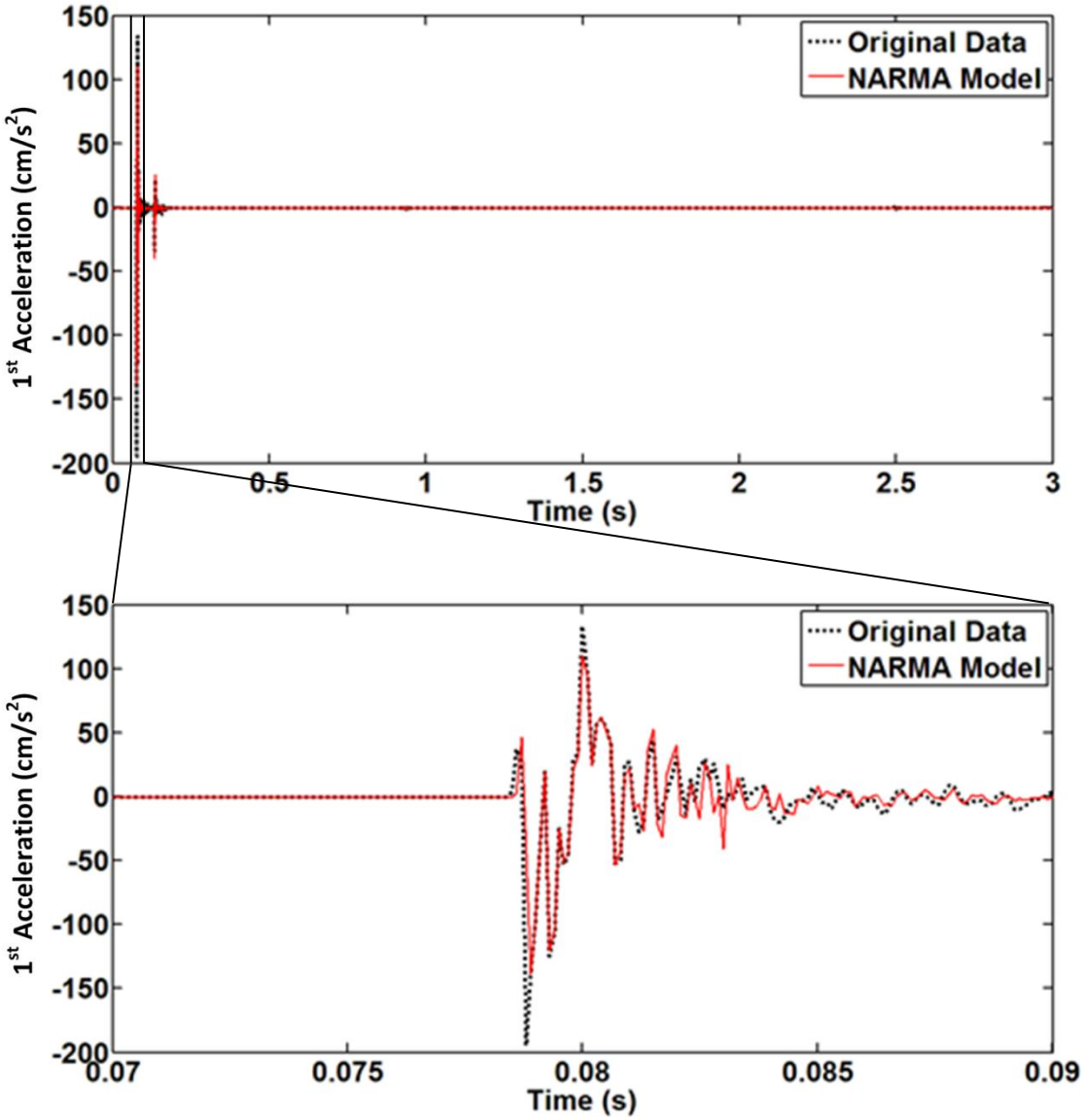

Figure 28. Comparison of the NARMA with the original data (worst case)

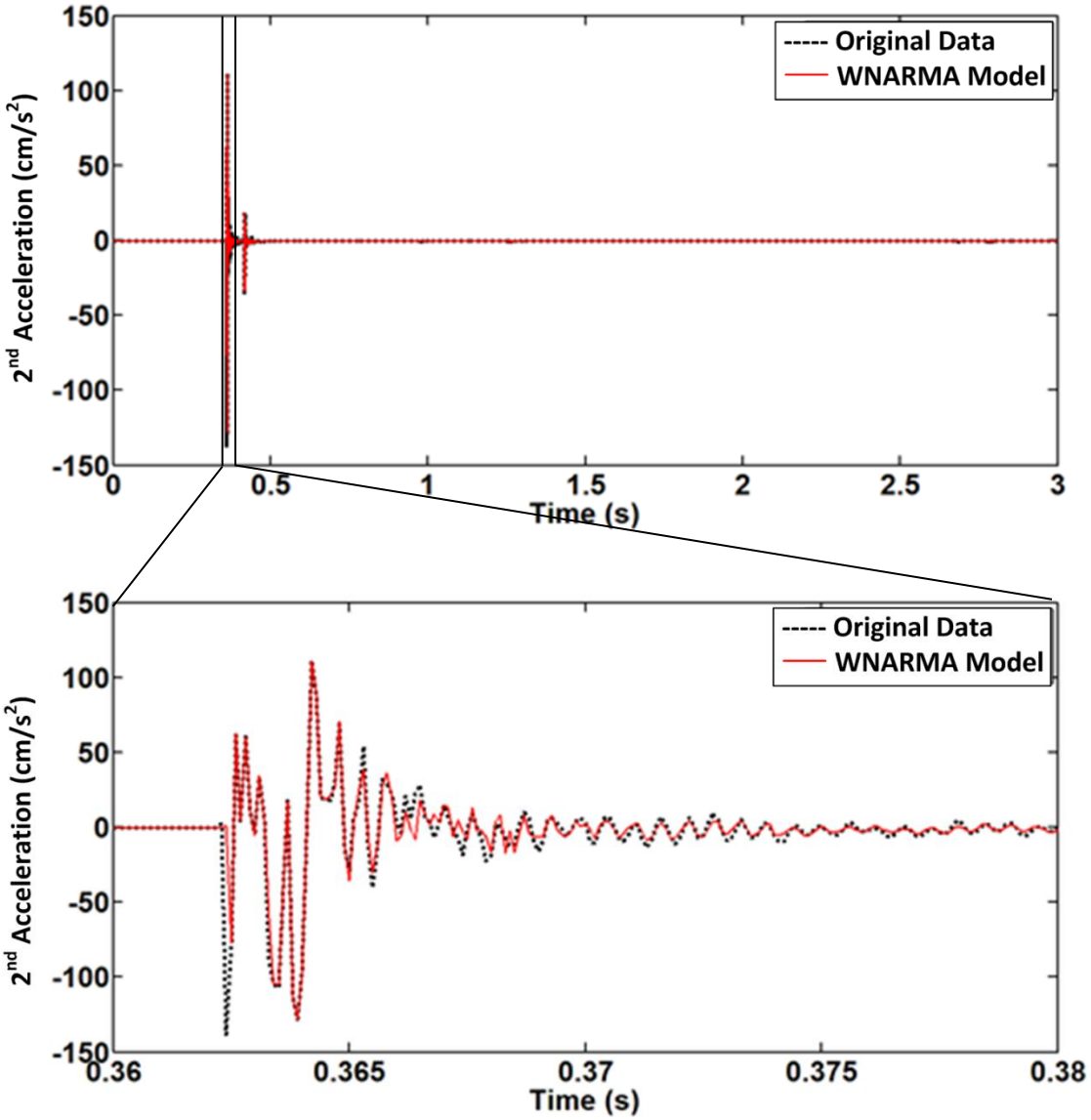

Figure 29. Comparison of the NARMA with the original data (worst case)

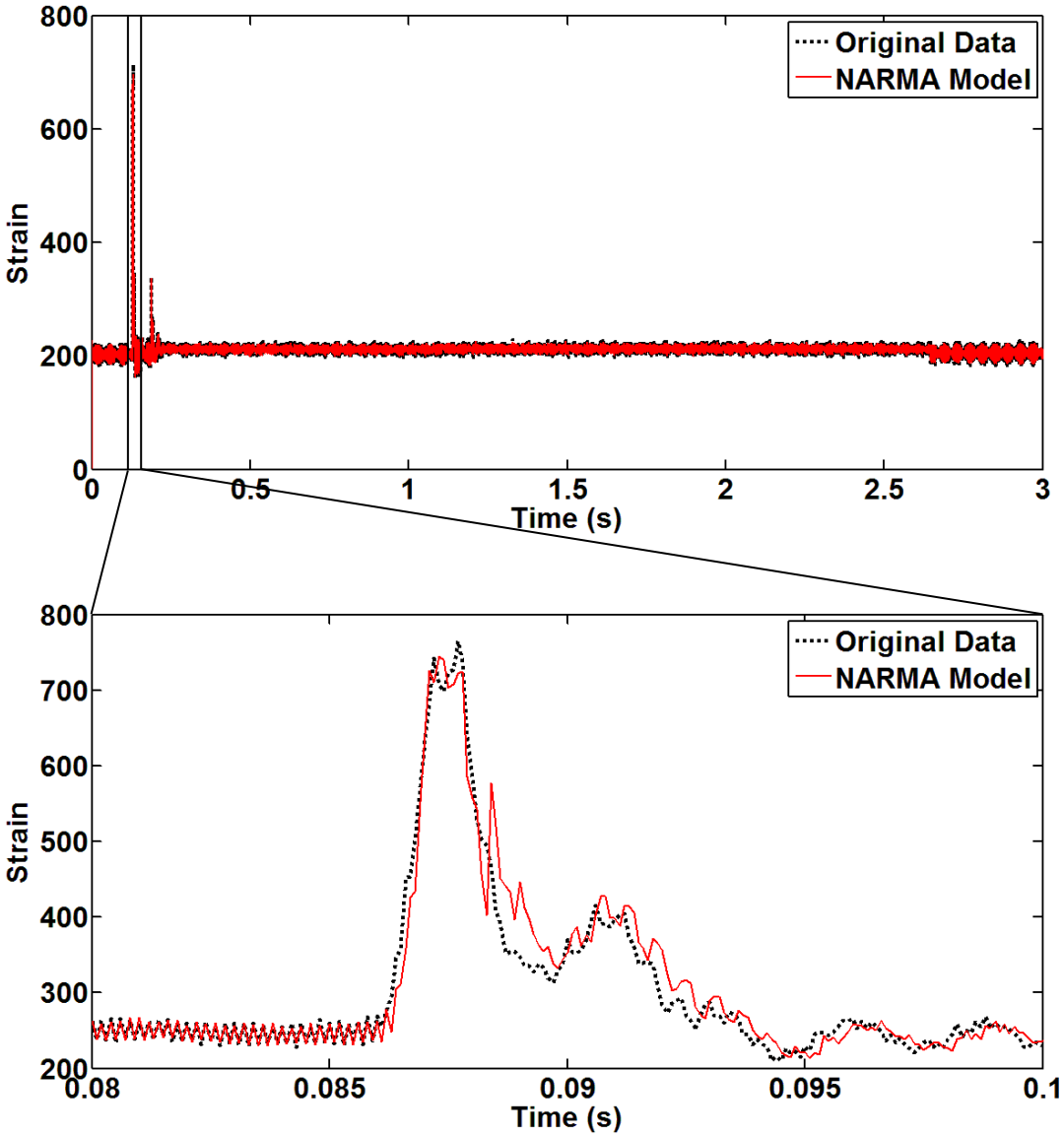

Figure 30. Comparison of the NARMA with the original data (worst case)

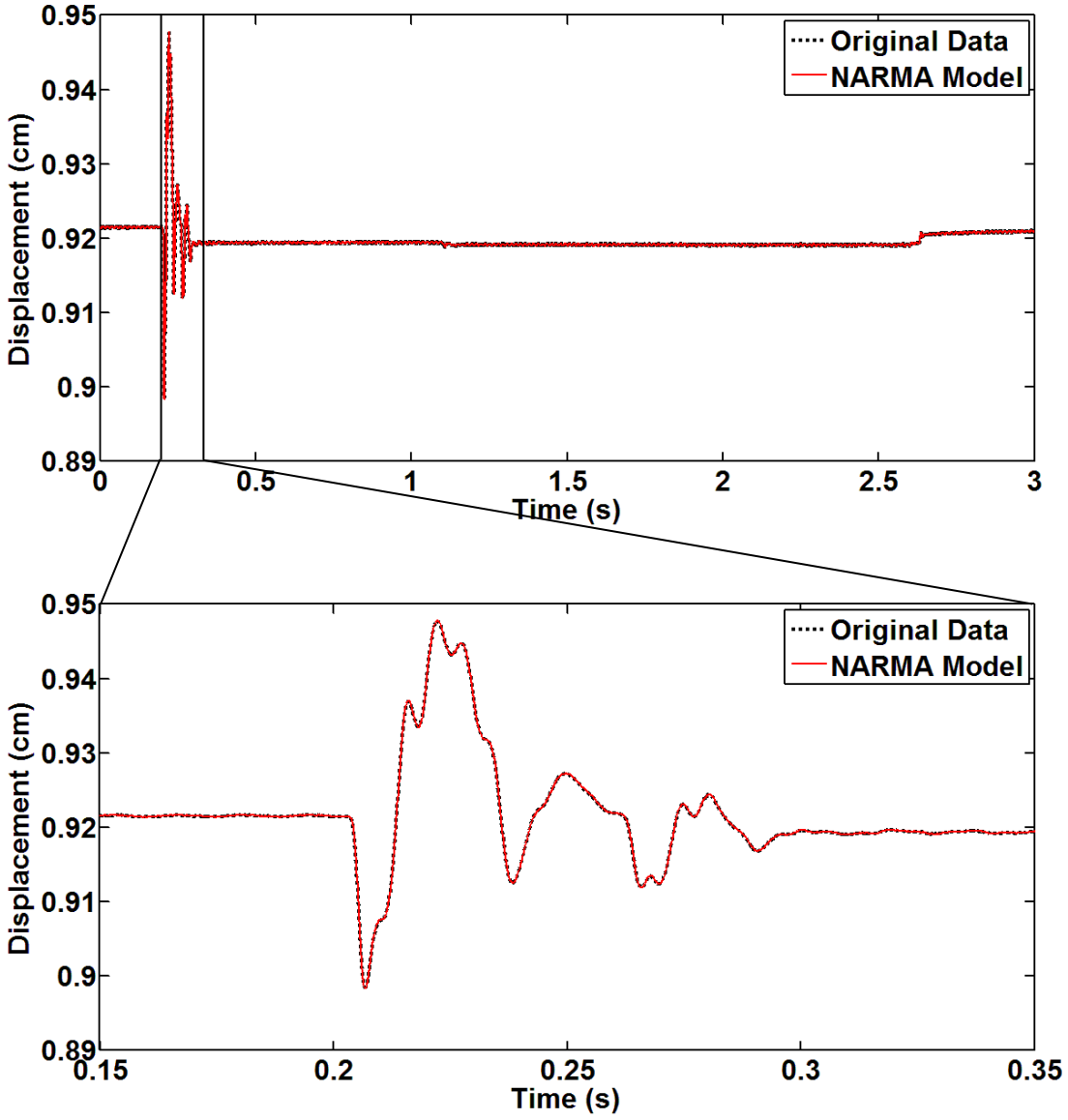

Figure 31. Comparison of the NARMA with the original data (worst case)

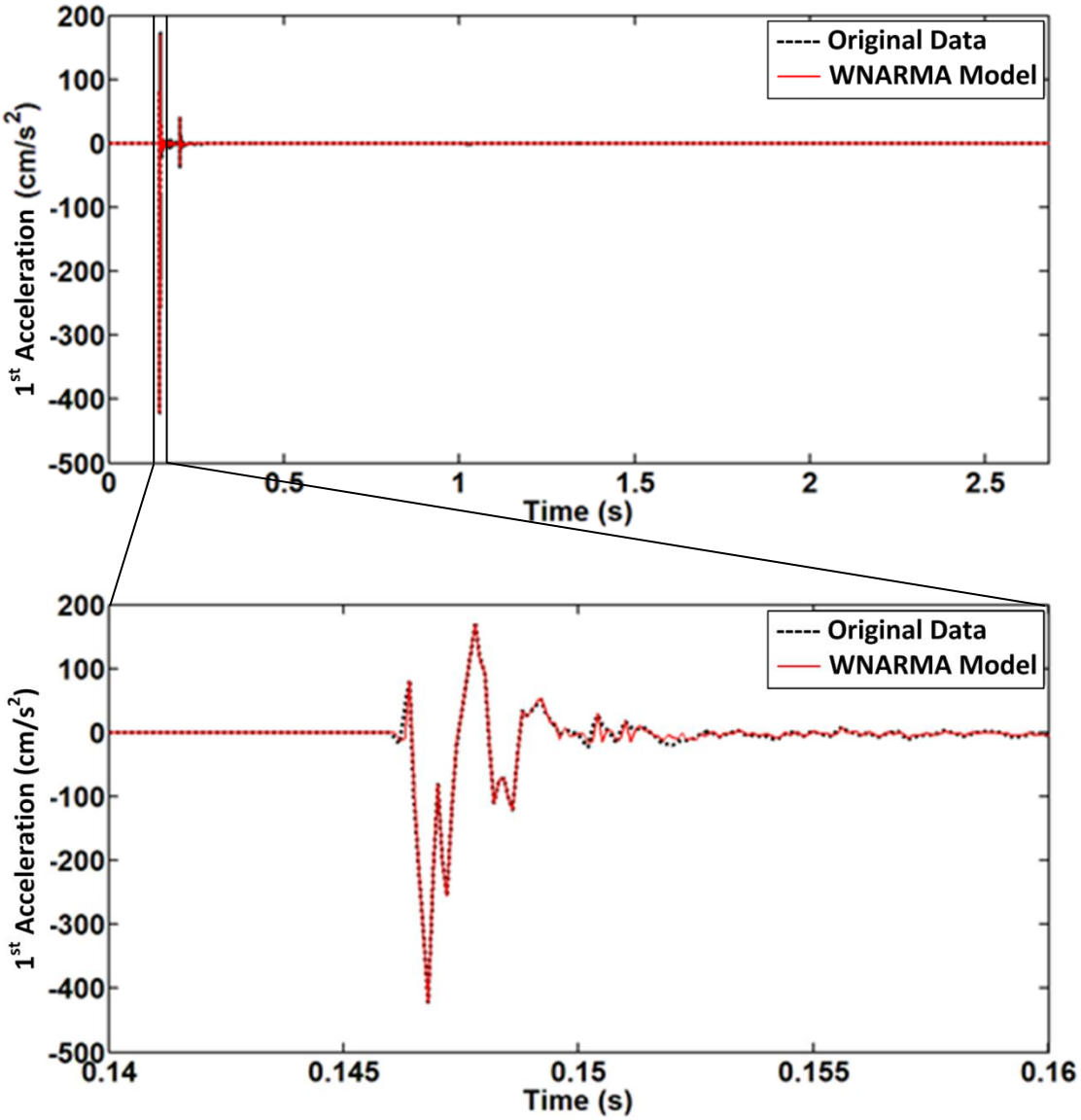

Figure 32. Comparison of the WNARMA with the original data (best case)

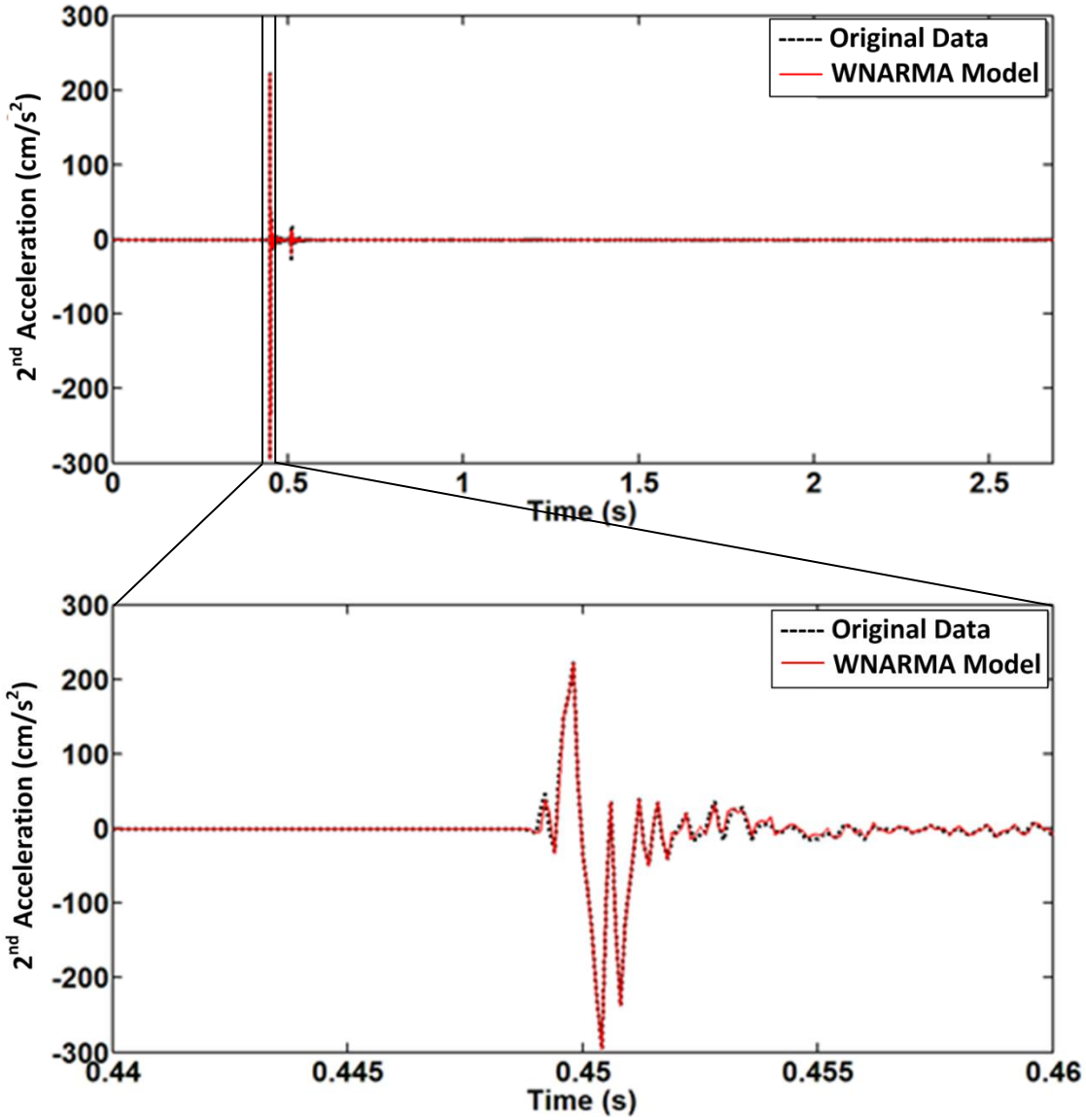

Figure 33. Comparison of the WNARMA with the original data (best case)

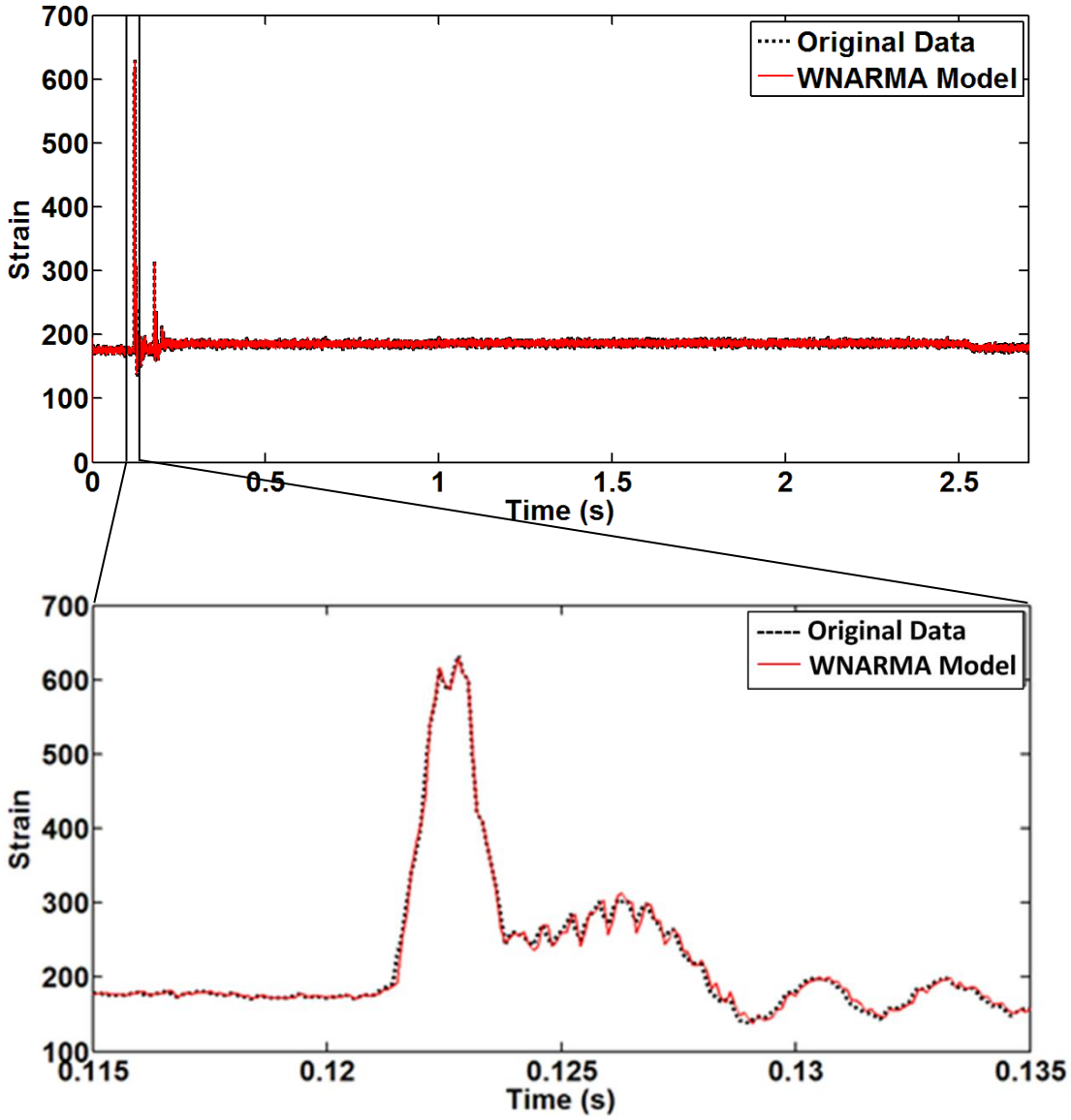

Figure 34. Comparison of the WNARMA with the original data (best case)

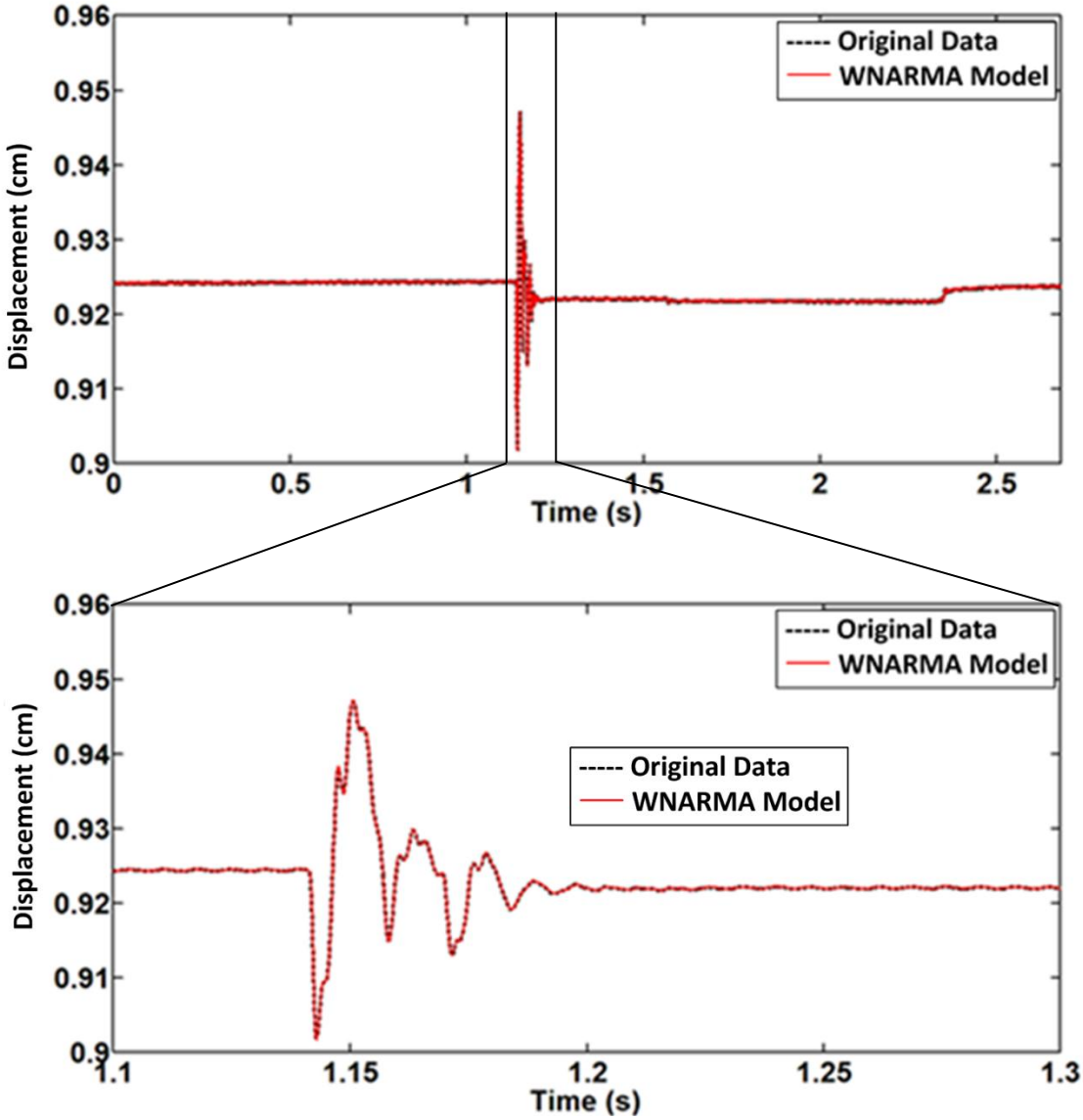

Figure 35. Comparison of the WNARMA with the original data (best case)

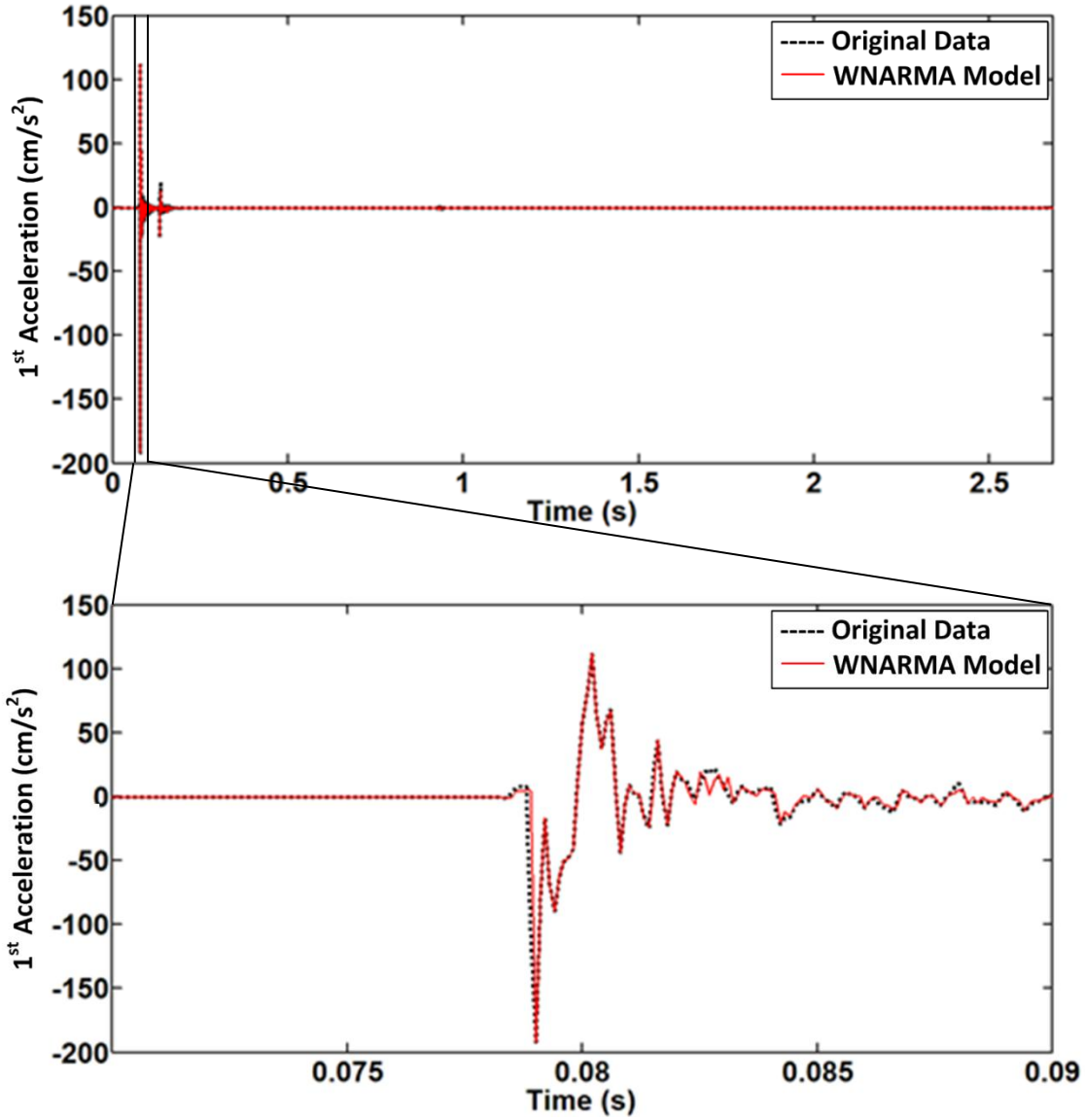

Figure 36. Comparison of the WNARMA with the original data (worst case)

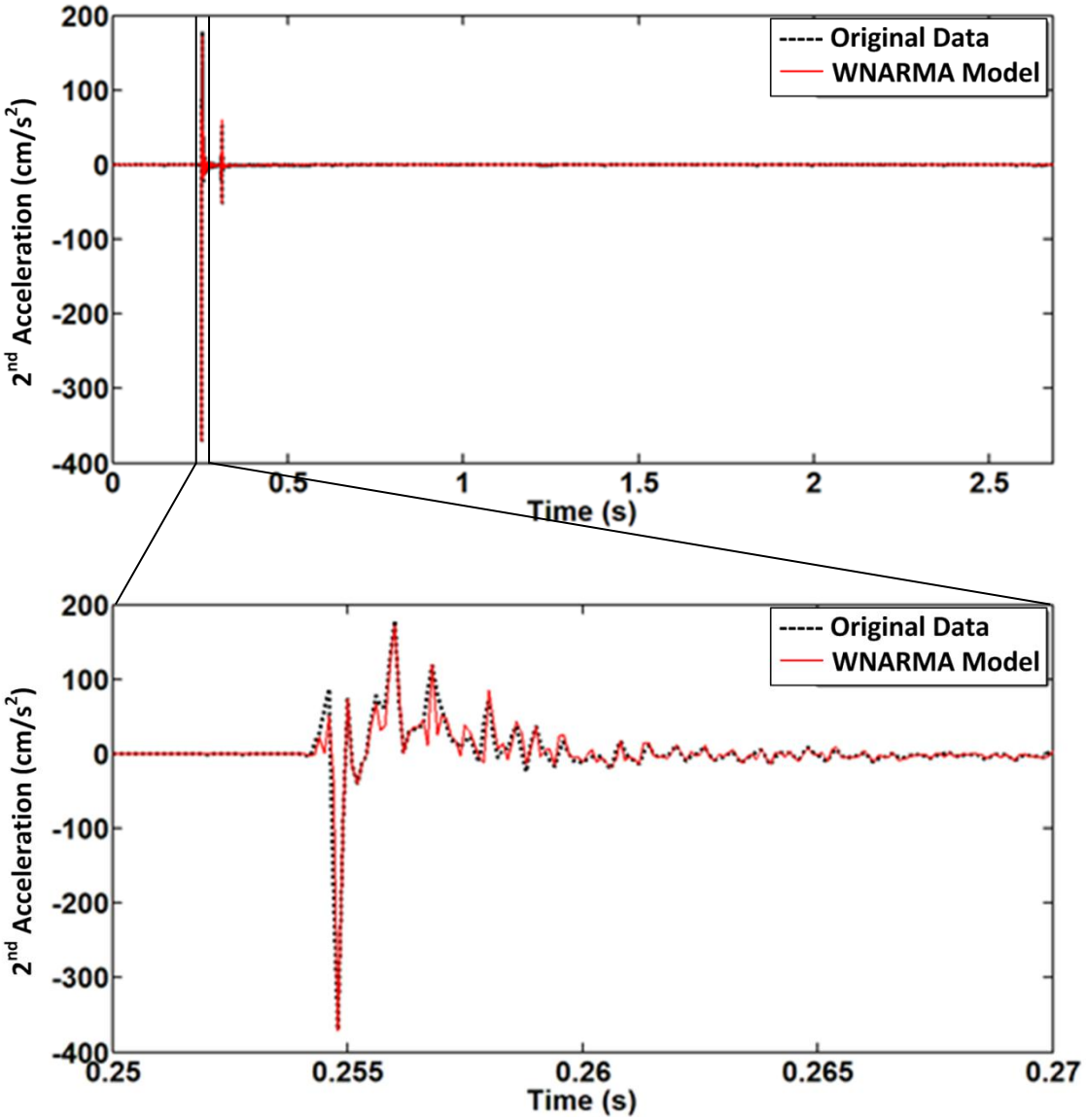

Figure 37. Comparison of the WNARMA with the original data (worst case)

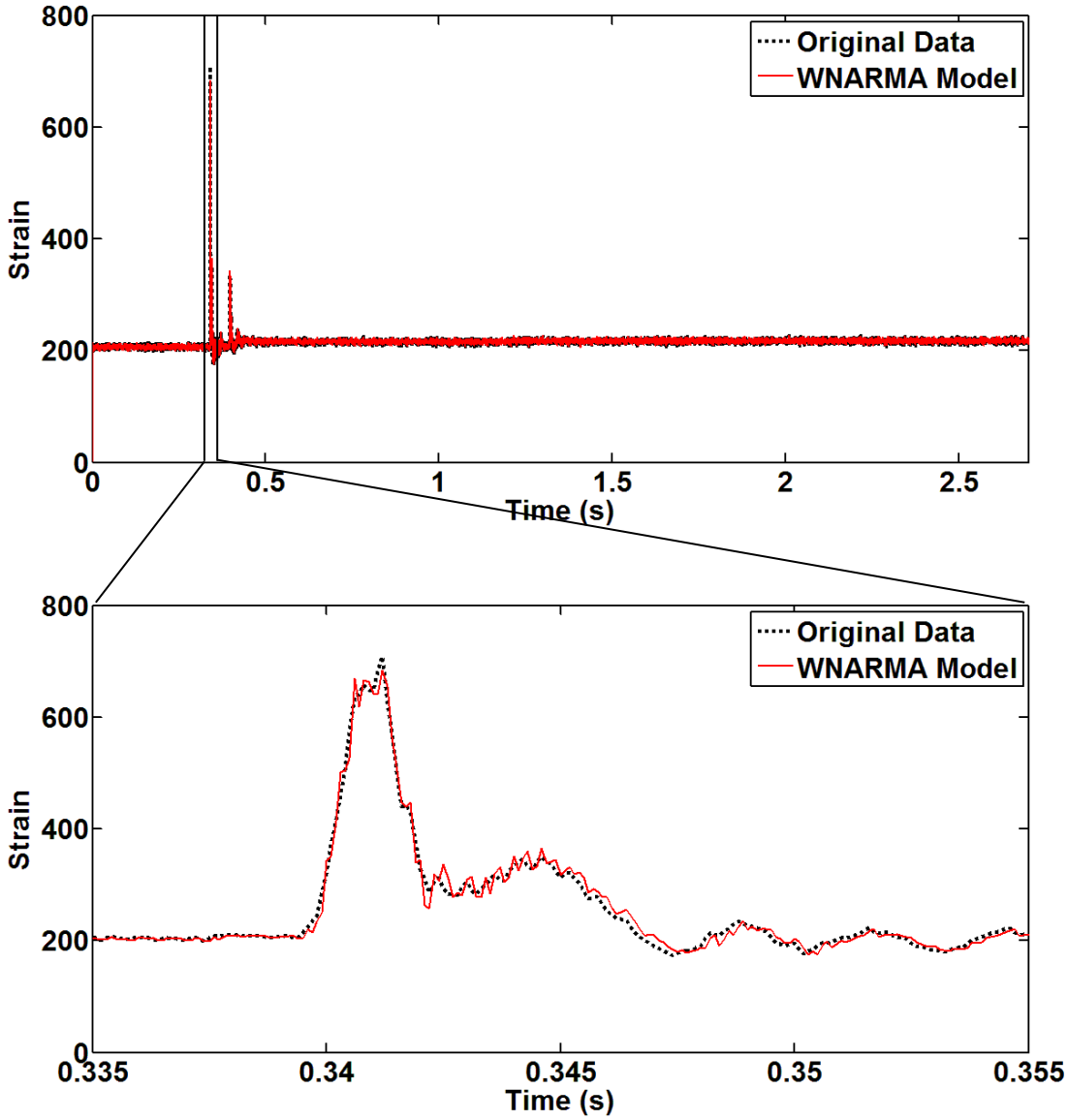

Figure 38. Comparison of the WNARMA with the original data (worst case)

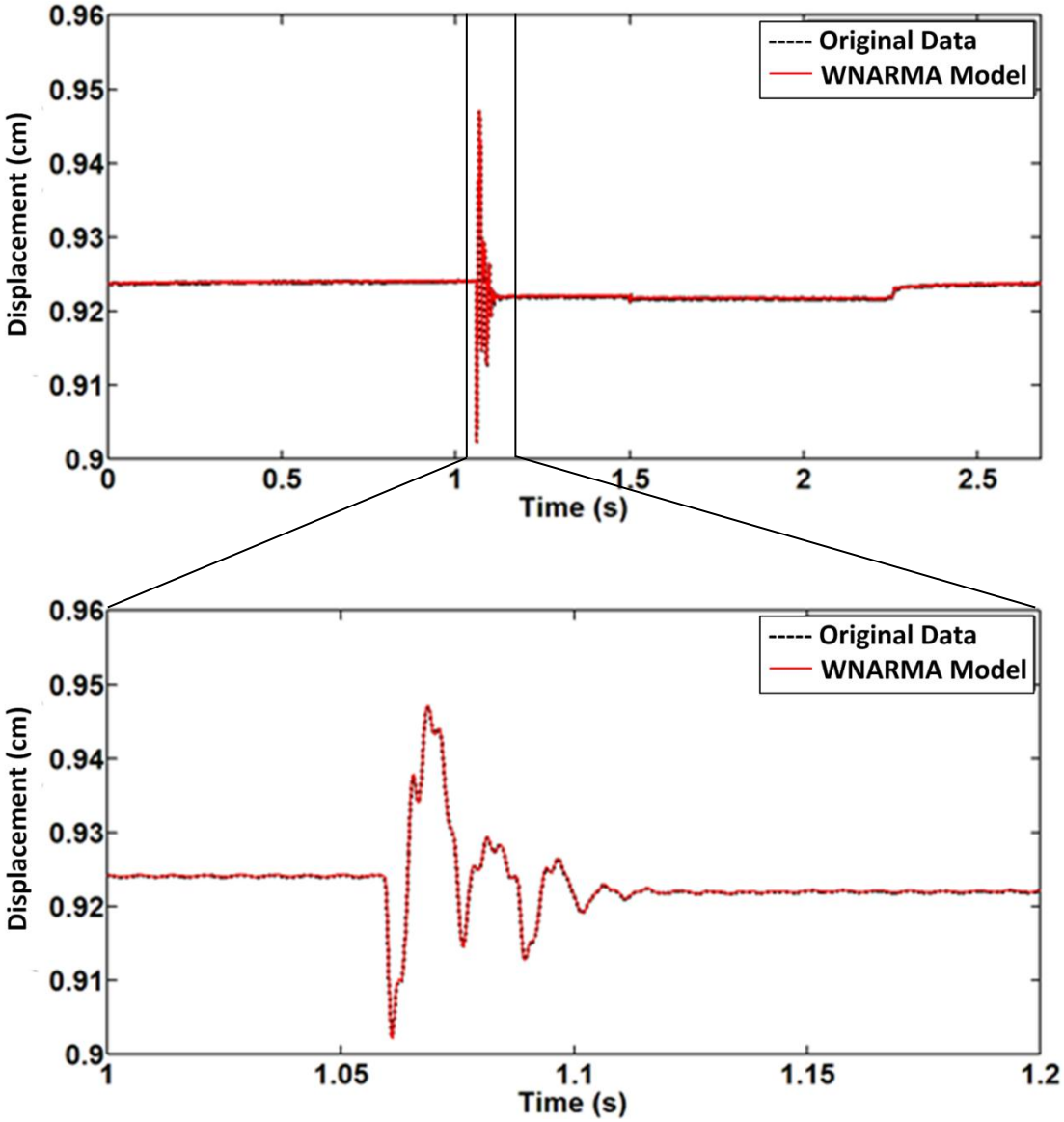

Figure 39. Comparison of the WNARMA with the original data (worst case)

In order to examine the performance of the trained models, it can be compared to the original response of the structure. Table 1 shows the training results in terms of the predefined parameters H_1-H_5 for NARMA model and WNARMA model. By comparing them, an estimated error between the two can be calculated. The first evaluation index, H_1, is

$$H_1 = max|\hat{y} - \tilde{y}| \tag{20}$$

where $\hat{y}$ is the estimation, $\tilde{y}$ is the actual structural response data. The second evaluation index, H_2, is

$$H_2 = min|\hat{y} - \tilde{y}| \tag{21}$$

As the third evaluation index, H_3, the root mean square error (RMSE) is considered and given by

$$H_3 = RMSE = \sqrt{\frac{\sum(|\hat{y} - \tilde{y}|)^2}{N}} \tag{22}$$

where N is the number of data points. As the forth evaluation index, H_4, the fitting rate (FR) is obtained by

$$H_4 = FR = \left[1 - \frac{|\tilde{y} - \hat{y}|}{|\tilde{y} - \bar{y}|}\right] \times 100 \tag{23}$$

where $\bar{y}$ is the mean value of the actual structural response data. If the designed model produces the same responses as the simulation model, FR is 100. The last evaluation index, H_5, is the computational load given by

$$H_5 = CPU\ time \tag{24}$$

Table 2 and 3 show the mesured average and 1-sigma values (also called one standard deviation), which are 1st acceleration, 2nd acceleration, strain, and displacement, obtained from 100 times of the impact tests; table 2 is from the NARMA model and tabel 3 is from the WNARMA model. As shown in Figure 40, over a wide range of percentage of the damage conditions from 0% to 50%, the WNARMA model shows better fitting rate (H_4) and overally less 1-sigma deviatons than the NARMA model. As shown in Figure 41, for all the damage conditions, the WNARMA model provides about 2 times faster computation times (H_5) than the NARMA model.

Table 2. Obtained H_1-H_5 using the NARMA model from 100 times of the impact tests

		1st Acceleration		2nd Acceleration		Strain		Displacement	
		Average	**1-sigma**	**Average**	**1-sigma**	**Average**	**1-sigma**	**Average**	**1-sigma**
H_1	Healthy	117.0132	41.36116	96.01462	44.20555	225.5615	24.15535	0.000462	2.55E-05
	Damage (5%)	107.7836	37.5862	90.79377	37.59041	256.6124	12.02564	0.000503	7.58E-05
	Damaged (10%)	106.7394	28.14828	94.39788	35.41153	268.1456	10.46993	0.000566	0.000127
	Damaged (15%)	95.80261	29.49449	77.01367	29.2855	271.7739	9.891383	0.000582	0.000110
	Damaged (30%)	102.641	33.94952	91.35975	31.78045	266.0078	10.8323	0.000559	9.17E-05
	Damaged (50%)	97.03043	27.33846	104.862	77.19517	276.3189	10.30786	0.000556	0.000116
H_2	Healthy	1.17E-05	1.48E-05	6.57E-06	7E-06	0.000152	0.000137	2.81E-09	3.33E-09
	Damaged (5%)	1.25E-05	1.51E-05	9.82E-06	1.07E-05	0.000143	0.000143	6.85E-09	1.80E-08
	Damaged (10%)	8.93E-06	1.12E-05	6.84E-06	7.83E-06	0.000196	0.000197	2.99E-06	3.83E-08
	Damaged (15%)	8.04E-06	8.21E-06	6.1E-06	6.88E-06	0.000174	0.000155	2.63E-08	3.24E-08
	Damaged (30%)	8.1E-06	9.02E-06	6.39E-06	9.07E-06	0.000162	0.000185	2.49E-08	3.24E-08
	Damaged (50%)	6.6E-06	6.78E-06	4.93E-06	5.68E-06	0.000162	0.000152	3.09E-08	4.90E-08
H_3	Healthy	1.004911	0.189768	0.852284	0.190584	4.351976	0.439396	4.43E-05	2.52E-07
	Damaged (5%)	1.108355	0.147489	1.006435	0.143464	4.869164	0.142063	5.65E-05	5.51E-05

	Damaged (10%)	1.305673	0.126264	1.225963	0.161423	5.513221	0.103888	0.000128	0.000102
	Damaged (15%)	1.092159	0.132445	1.021768	0.13993	5.303744	0.189692	0.000140	0.000108
	Damaged (30%)	1.262892	0.171116	1.14496	0.167894	5.17707	0.120169	0.000122	8.52E-05
	Damaged (50%)	1.213648	0.181166	1.200916	0.654956	5.224984	0.136119	0.000125	8.69E-05
H_4	Healthy	91.97536	4.569571	92.82258	3.423898	93.53895	1.336201	99.95917	0.007120
	Damaged (5%)	89.81089	5.240733	83.84788	7.073795	94.90744	0.471279	99.97409	0.000112
	Damaged (10%)	83.89015	8.861433	77.05857	7.140653	95.45787	0.272238	99.96726	0.000278
	Damaged (15%)	84.57976	7.387826	80.4448	6.272009	95.37502	0.276808	99.96084	0.000352
	Damaged (30%)	86.27719	8.94987	79.3123	8.297836	95.41766	0.397506	99.96665	0.000260
	Damaged (50%)	83.64854	8.212511	80.10675	6.834474	95.77997	0.283354	99.96617	0.000274
H_5	Healthy	6.017949	0.122715	6.071465	0.125472	6.143931	0.123616	5.977546	0.117251
	Damaged (5%)	6.125412	0.132541	6.351453	0.127719	6.451255	0.126754	6.211542	0.120421
	Damaged (10%)	6.089015	0.114852	6.158574	0.119723	6.457872	0.132445	6.089903	0.122312
	Damaged (15%)	6.18976	0.127845	6.474798	0.121714	6.675023	0.120542	6.210552	0.130784
	Damaged (30%)	6.277192	0.119224	6.312304	0.131795	6.617655	0.121551	6.278027	0.127712
	Damaged (50%)	6.348543	0.172755	6.406747	0.122645	6.779968	0.129431	6.309476	0.125915

Table 3. Obtained H_1-H_5 using the WNARMA model from 100 times of the impact tests

		1st Acceleration		2nd Acceleration		Strain		Displacement	
		Average	**1-sigma**	**Average**	**1-sigma**	**Average**	**1-sigma**	**Average**	**1-sigma**
H_1	Healthy	74.15566	32.59813	64.74309	24.52397	226.2095	22.49667	0.000436	2.21E-05
	Damage (5%)	61.32611	26.26592	55.94566	22.58485	256.5325	6.160928	0.000484	5.94E-05
	Damaged (10%)	59.03297	22.19288	56.57697	19.01703	267.0786	5.312705	0.000634	0.000102
	Damaged (15%)	54.9399	22.10074	48.36461	20.36118	272.0261	6.703196	0.000883	7.02E-05
	Damaged (30%)	57.9794	22.73076	56.31486	19.71523	264.6474	5.288627	0.000606	0.000115
	Damaged (50%)	60.83789	25.28855	58.8489	35.57451	277.3487	5.477267	0.000664	0.000111
H_2	Healthy	6.16E-07	5.75E-07	7.03E-07	8.3E-07	5.6E-05	4.96E-05	5.35E-10	8.72E-10
	Damaged (5%)	5.62E-07	6.17E-07	4.53E-07	4.06E-07	5.59E-05	6.28E-05	1.48E-09	7.56E-09
	Damaged (10%)	4.61E-07	4.28E-07	5.41E-07	7.15E-07	7.08E-05	8.57E-05	3.37E-08	4.07E-08
	Damaged (15%)	5.81E-07	5E-07	4.89E-07	5.41E-07	6.62E-05	6.6E-05	1.65E-08	2.95E-08
	Damaged (30%)	5.07E-07	4.68E-07	4.12E-07	4.15E-07	5.21E-05	4.87E-05	2.51E-08	4.42E-08
	Damaged (50%)	4.81E-07	6.57E-07	4.89E-07	8.38E-07	5.13E-05	5.46E-05	3.86E-08	4.43E-08
H_3	Healthy	0.712237	0.198694	0.629289	0.162255	2.629492	0.415372	2.18E-05	2.32E-07
	Damaged (5%)	0.674378	0.144632	0.65569	0.129579	3.206492	0.159142	2.79E-05	4.26E-05
	Damaged (10%)	0.713901	0.114363	0.731584	0.097484	3.663352	0.12688	0.000108	8.73E-05
	Damaged (15%)	0.597681	0.111137	0.603096	0.096308	4.230383	0.331616	7.15E-05	7.62E-05
	Damaged (30%)	0.721912	0.143451	0.705317	0.110583	3.400553	0.133669	0.000105	9.81E-05
	Damaged (50%)	0.658441	0.123336	0.698957	0.303492	3.454806	0.13088	0.000127	9.53E-05
H_4	Healthy	95.4284	2.636054	95.04278	2.984552	98.83698	0.480298	99.99016	0.001751
	Damaged (5%)	95.70797	2.410087	91.45105	3.300479	98.81752	0.287094	99.99257	0.001162

	Damaged (10%)	94.26451	3.188385	89.07528	3.443394	98.61668	0.192286	99.9742	0.002144
	Damaged (15%)	94.23094	2.910489	90.81493	2.54996	99.55214	0.311955	99.97927	0.002146
	Damaged (30%)	94.71686	3.788815	89.72437	3.430392	98.75491	0.244442	99.97398	0.002466
	Damaged (50%)	93.78065	3.209989	90.21825	3.214821	98.66726	0.173323	99.96798	0.002936
H_5	Healthy	3.245154	0.10291	3.015481	0.103414	3.112154	0.106348	3.001585	0.101188
	Damaged (5%)	3.125415	0.09979	3.151569	0.102407	3.172145	0.107373	3.121456	0.101245
	Damaged (10%)	3.254156	0.105344	3.215415	0.103216	3.321456	0.107442	3.182145	0.101344
	Damaged (15%)	3.365441	0.103178	3.144445	0.102988	3.214561	0.107405	3.165541	0.100327
	Damaged (30%)	3.178424	0.104354	3.321451	0.102607	3.221445	0.107416	3.201445	0.100345
	Damaged (50%)	3.295125	0.102889	3.214459	0.102916	3.298412	0.101659	3.218554	0.101317

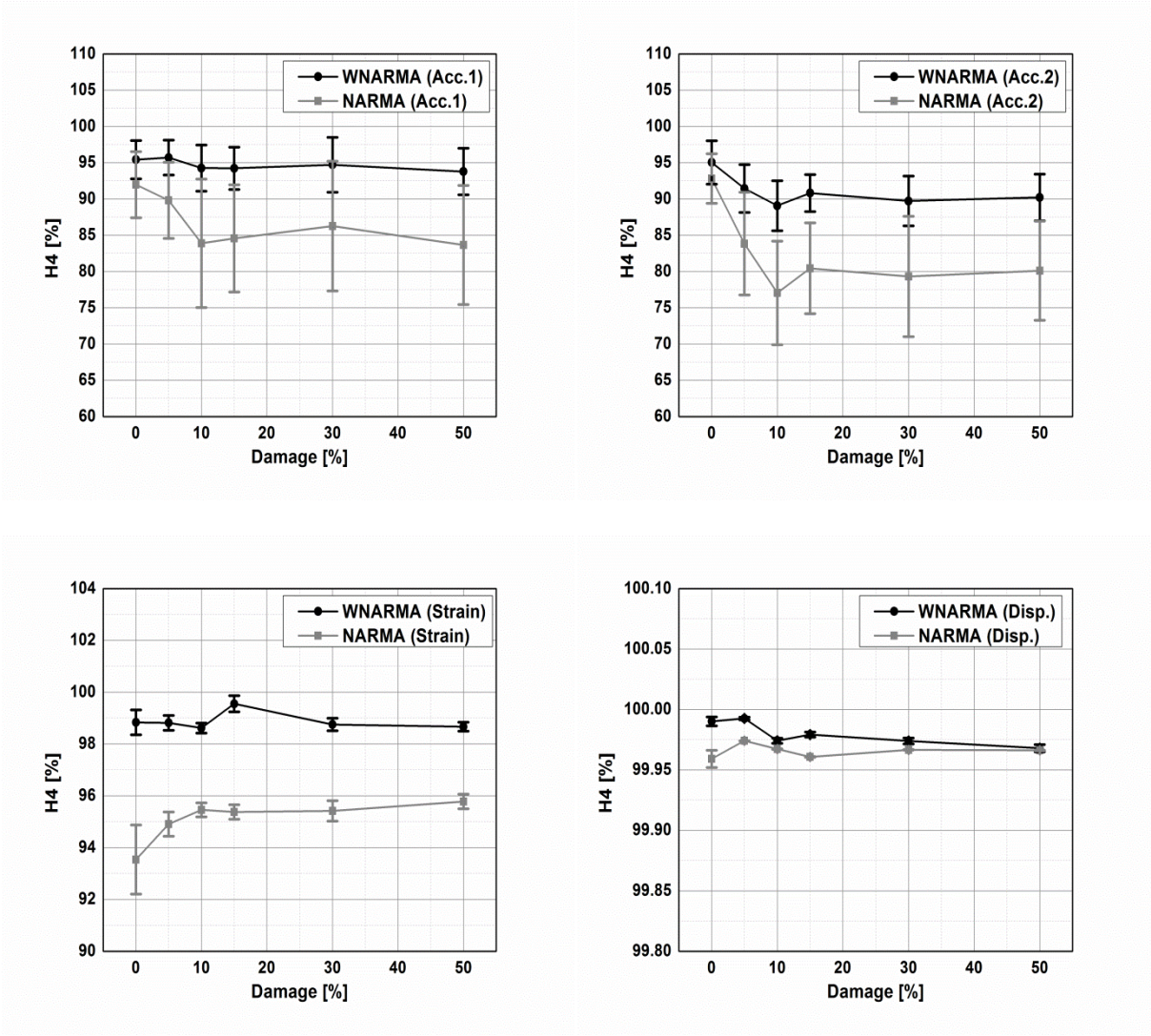

Figure 40. Average and 1-sigma of H_4 (fitting rate) of WNARMA and NARMA models from 100 times of the impact tests (a) 1st acceleration (b) 2nd acceleration (c) strain (d) displacement

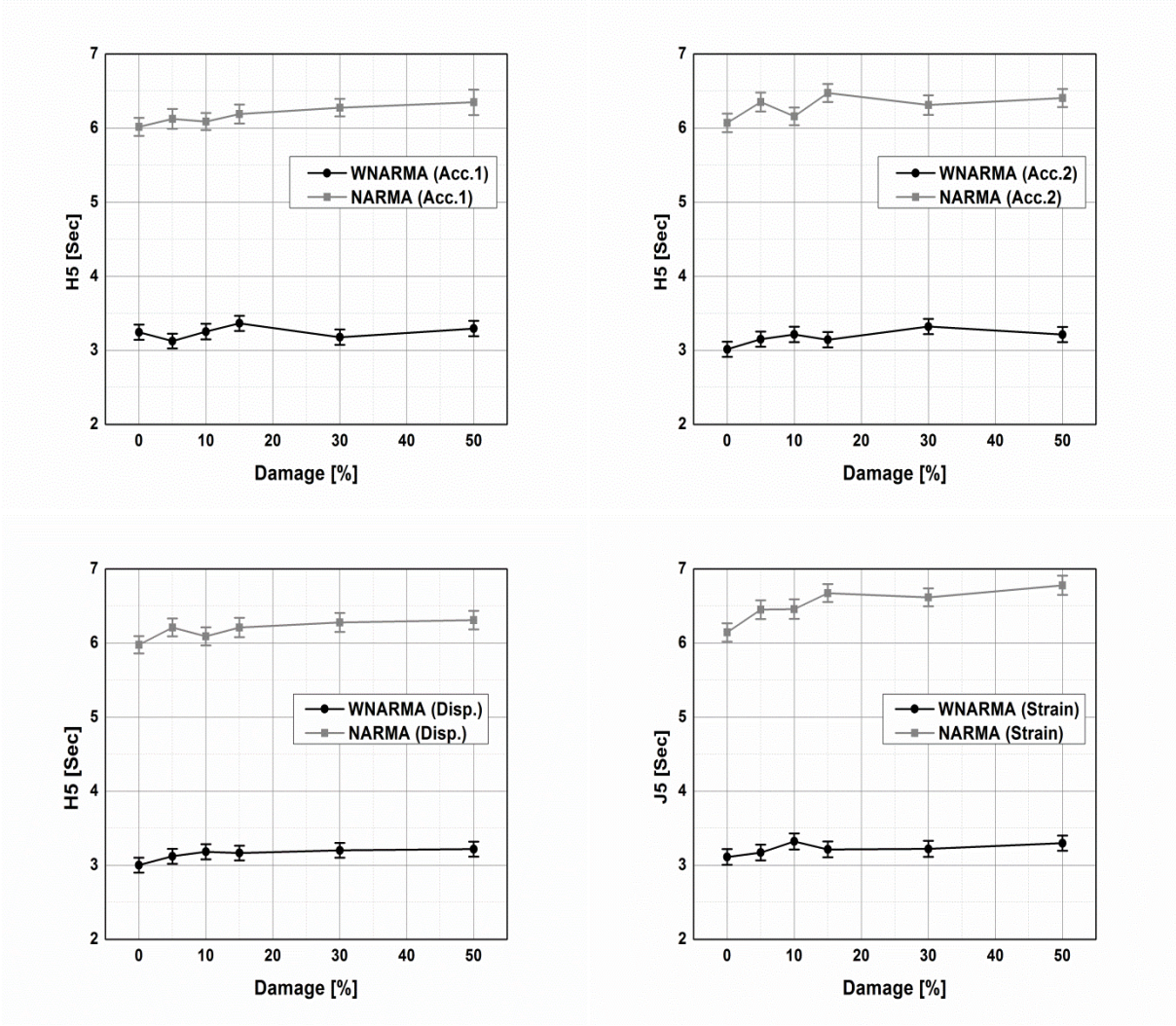

Figure 41. Average and 1-sigma of H_5 (computation time) of WNARMA and NARMA models from 100 times of the impact tests (a) 1st acceleration (b) 2nd acceleration (c) strain (d) displacement

3.2.4. Conclusion

In this paper, a wavelet based nonlinear autoregressive moving average (WNARMA) time series model is proposed for system identification (SI) of smart concrete structures subjected to high impact loads. For a case study, a reinforced concrete equipped with a magneto-rheological (MR) damper is selected, and the dynamic response of the structure is obtained from an experimental study using a drop tower test. From the 100 times of the impact tests, the WNARMA model shows

better fitting rate and less one-standard deviations than the NARMA model over a wide range of percentage of the damage conditions from 0% to 50%. In addition, the WNARMA model provides about 2 times faster computation times (H_5) than the NARMA model for all the damage conditions.

4. Summary

In this thesis, a wavelet based nonlinear autoregressive moving average (WNARMA) time series model is proposed for system identification (SI) of smart steel structures subjected to ambient excitation and smart concrete structures under high impact loads. To demonstrate the effectiveness of the wavelet-based NARMA modeling (WNARMA), two case studies are conducted. First case study is conducted for SI of a three-story building employing an MR damper under ambient excitation, and for second case study, the experimental study is performed for SI of a reinforced concrete structure employing an MR damper under a high impact load. The simulation results show that the computation of the WNARMA model is faster than that of the NARMA model without sacrificing the modeling accuracy. In addition, the WNARMA model is robust against noise in the data since it inherently has a denoising capacity.

5. Future works

Throughout this research, the effectiveness of the WNARMA model has been proven for the use in system identification (SI) of a three-story steel smart structure under ambient excitation and a reinforced smart concrete structure under high impact loads. Both structures are equipped with an MR damper which is one of the promising semi-active control devices for structural vibration reduction that combines the best features of both active and passive control systems.

It is expected that the effectiveness of the WNARMA model can be extended to other smart structure systems under various input sources. It would be interesting to study the prediction of the structural response to further excitation in addition of damage detection. This research could be expanded to the application of damage detection using the residual error, which is the difference between the original signal and predicted signal; the error will increase when the damage occurs in the structure. In addition, it would be attractive to build a real time control system of smart structures with the proposed WNARMA model.

.

6. Reference

[1] H. Adeli and X. Jiang, "Dynamic fuzzy wavelet neural network model for structural system identification," *Journal of Structural Engineering,* vol. 132, no. 102, pp. 102-111, 2006.

[2] P. Andersen, "Identification of civil engineering structures using vector ARMA models," Department of Building Techology and Structural Engineering, Aalborg University, Denmark, 1997.

[3] N. S. Bajaba and K. A. Alnefaie, "Multiple damage detection in structures using wavelet transforms," *Emirates Journal for Engineering Research,* vol. 10, no. 1, pp. 35-40, 2005.

[4] K. Bani-Hani, J. Ghaboussi and S. P. Schneider, "Experimental study of identification and control of structures using neural network, Part1: identification," *Earthquake Engineering and Strcutral Dynamics,* vol. 28, no. 9, pp. 995-1018, 1999.

[5] R. Brincker, P. H. Kirkegaard and P. Andersen, "Damage detection in an offshore structure," in *Proceedings of the 13th International Modal Analysis Conference*, Nashville, Tennessee, 1995.

[6] R. Brincker, P. Andersen, P. H. Kirkegaard and J. P. Ulfkjaer, "Damage detection in laboratory concrete beams," in *Proceedings of the 13th International Modal Analysis Conference*, Nashville, Tennessee, 1995.

[7] R. Brincker, L. Zhang and P. Andersen, "Modal identification of output-only systems using frequency domain decomposition," *Smart Material and Structures,* vol. 10, no. 3, pp. 441-445, 2001.

[8] E. P. Carden and J. M. Brownjohn, "ARMA modelled time series classification for structural health monitoring," *Mechanical Systems and Signal Processing,* vol. 22, no. 2, pp. 295-314, 2007.

[9] C. Devriendt, P. Guillaume, E. Reynders and G. D. Roeck, "Operational modal analysis of a bridge using transmissibility measurements," in *Proceedings of the 25th International Modal Analysis Conference,* Orlando, FL, 2007.

[10] S. Dyke, B. S. Jr., M. Sain and J. Carlson, "Modeling and control of magnetorheological dampers for seismic response reduction," *Smart Materials and Structures,* vol. 5, no. 5, pp. 565-575, 1996.

[11] M. Ettefagh, M. Sadeghi and S.Khanmohammadi, "Structural damage detection, using fuzzy classification and ARMA parametric modeling," *Journal of Aerospace and Mechanical Engineering,* vol. 3, no. 2, pp. 85-98, 2007.

[12] H. Gokdag, "Wavelet-based damage detection method for beam-like structures," *Gazi University Journal of Science,* vol. 23, no. 3, pp. 339-349, 2010.

[13] M. Gul and F. N. Catbas, "A modified time series analysis for identification, localization, and

quantification of damage," in *Proceedings of the 27th International Modal Analysis Conference*, Orlando, FL, 2009.

[14] Z. Hasiewicz and M. Pawlak, "Nonlinear system identification via wavelet expansions," in *Proceedings Symposium on System Identification (SYSID)* , Santa Barbara, CA, 2000.

[15] M. A. Hogg and S. Tindale, Blackwell handbook of social psychology: group pocesses, Oxford, UK: Blackwell Publishers, 2008.

[16] S. R. Horton, M. M. R. Taha and T. J. Baca, "A neural-wavelet damage detection module for structural health monitoring," in *Structural Health Monitoring 2005*, Lancaster, PA, DEStech Publicatios, 2005, pp. 556-564.

[17] Z. Hou, M. Noori and R. S. Arnand, "Wavelet-based approach for structural damage detection," *Journal of Engineering Mechanics,* vol. 126, no. 7, pp. 665-777, 2000.

[18] N. F. Hunter, "Analysis of nonlinear systems using ARMA models," in *Proceedings of the 8th International Modal Analysis Conference,* 1990.

[19] G. H. James III, T. G. Came and R. L. Mayes, "Modal parameter extraction from large operating structrues using ambient exciation," in *Proceedings of the 14th International Modal Analysis Conference*, Bethel, CT, 1996.

[20] O. R. John, Multivariable control for industrial applications, London, UK: Peter Peregrinus Ltd, 1987.

[21] G. Kerschen, K. Worden, A. F. Vakakis and J.-C. Golinwal, "Past, present and future of nonlinear system identification in structural dynamics," *Mechanical System and Signal Processing,* vol. 20, no. 3, pp. 505-592, 2006.

[22] C. H. Loh, C. Y. Lin and C. C. Huang, "Time domain identification of frame under earthquake loadings," *Journal of Engeering Mechanics,* vol. 126, no. 7, pp. 693-703, 2000.

[23] H. Zheng and A. Mita, "Damage indicator defined as the distance between ARMA models for structural health monitoring," *Structrual Control and Health Monitoring,* vol. 15, no. 7, pp. 992-1005, 2008.

[24] H. B. Yun, S. F. Masri and J. P. Caffrey, "Stochastic change detection in uncertain nonlinear systems using data-driven sytem identification method," in *The 26th IMAC on Conference and Expositon on Structural Dynamics*, Orlando, FL, 2008.

[25] F. Yi, J. S. Dyke, M. J. Caicedo and D. Carlson, "Experimental verification of multi-input seismic control strategies for smart dampers," *ASCE Journal of Engineering Mechanics,* vol. 127, no. 11, pp. 1152-1164, 1999.

[26] M. J. Whelan, M. V. Gangone, K. D. Janoyan and R. Jha, "Real-time wireless vibration monitoring for operational modal analysis of an integral abutment highway bridge," *Engineering Structures,* vol. 31, no. 10, pp. 2224-2235, 2009.

[27] I. Takewaki, M. Nakamura and S. Yoshitomi, System identification for structural health monitoring, Billerica, MA: WIT Press, 2012.

[28] H. W. Song and W. L. Wang, "Non-linear system identification using frequency domain measurement data," in *Proceedings of the 16th International Modal Analysis Conference*, Santa Barbara, CA, 1998.

[29] H. Sohn, J. A. Czarnecki and C. R. Farrar, "Structural health monitoring using statistical process control," *Journal of Structural Engineering,* vol. 126, no. 11, pp. 1356-1363, 2000.

[30] H. Sohn and C. R. Farrar, "Statistical process control and projection techniques for structural health monitoring," in *Proceedings of European COST F3 Conference on Sytem Identification and Structural Health Monitoring*, Madrid, Spain, 2000.

[31] S. d. Silva, M. D. Junior, V. L. Junior and M. J. Brennan, "Structural damage detection by fuzzy clustering," *Mechanical Systems and Singnal Processing,* vol. 22, no. 7, pp. 1636-1649, 2008.

[32] C. G. d. Silva, "Time-series forecasting with a non-linear model and the scatter search meta-heuristic," *Information Sciences,* vol. 178, no. 16, pp. 3288-3299, 2008.

[33] A. Rytter, J. L. Jensen and P. Hansen, "System identification from output measurements," in *Proceedings of the 8th International Modal Analysis Conference*, Orlando, FL, 1990.

[34] M. Rucka, "Damage detection in beams using wavelet transform on higher vibration modes," *Journal of Theoretical and Applied Mechanics,* vol. 49, no. 2, pp. 339-417, 2011.

[35] W. X. Ren and Z. H. Zong, "Output-only modal parameter identification of civil engineering structures," *Structrual Engineering and Mechanics,* vol. 17, no. 3-4, pp. 429-444, 2004.

[36] E. Parloo, P. Verboven, P. Guillaume and M. Overmeire, "Force identification by means of in-operation modal models," *Journal of Sound and Vibration,* vol. 262, no. 1, pp. 161-173, 2003.

[37] A. Nishitani, N. Yamada and S. Yamada, "Structural system identification with active mass damper used for providing input excitation," in *The 11th World Conference on Earthquake Engineering*, Tokyo, Japan, 1996.

[38] M. Nakamura, S. F. Masri, A. G. Chassiakos and T. K. Caughey, "A method for non-parametric damage detection through the use of neural networks," *Earthquake Engineering Structural Dynamics,* vol. 27, no. 9, pp. 997-1010, 1998.

[39] K. K. Nair, A. S. Kiremidjian and K. H. Law, "Time series-based damage detection and localization algorithm with application to the ASCE benchmark structure," *Jounal of Sound and Vibration,* vol. 291, no. 2, pp. 349-368, 2006.

[40] K. K. Nair and A. S. Kiremidjian, "Time series based structural damage detection algorithm using gaussian mixtures modeling," *Journal of Dynamic Systems, Measurement, and Control,* vol. 129, no. 3, pp. 285-293, 2007.

[41] A. Mosavi, D.Dickey, R.Seracino and S.Rizkalla, "Identifying damage locations under ambient vibrations utilizing vector autoregressive models and Mahalanobis distances," *Mechanical Systems and Signal Processing,* vol. 26, no. 1, pp. 254-267, 2011.

[42] S. Lu, K. H. Ju and K. H. Chon, "A new algorithm for linear and nonlinear ARMA model parameter estimation using affine geometry," *IEEE Transactions on Biomedical Engineering,* vol. 48, no. 10, pp. 1116-1124, 2001.

[43] K. C. Lu, C. H. Loh, Y. S. Yang, J. P. Lynch and K. H. Law, "Real-time structural damage detection using wireless sensing and monitoring system," *Smart Structures and Systems,* vol. 4, no. 6, 2008.

[44] C. H. Loh and J. Y. Duh, "Analysis of nonlinear system using NARMA models," in *Proceedings of JSCE: Structural Engineering/Earthquake Engineering,* Tokyo, Japan, 1996.

[45] Y. Lei and Y. Wu, "Non-parametric identification of structural nonlinearity with limited input and output measurements," *Advanced Materials Research,* Vols. 243-249, pp. 5403-5407, 2011.

[46] Y. Lei, A. S. Kiremidjian, K. K. Nair, J. P. Lynch and K. H. Law, "Time synchronization algorithms for wireless monitoring system," in *Proceedings of SPIE 10th Annual International Symposium on Smart Structures and Materials,* San Diego, CA, 2003.

[47] T. H. Le and Y. Tamura, "Modal identification of ambient vibration structure using frequency domain decomposition and wavelet transform," in *The 7th Asia-Pacific Conference on Wind Engineering,* Taipei, Taiwan, 2009.

[48] J. Kullaa and T. Tirkkonen, "System identification of a bridge from response data comprising spurious harmonics," in *Proceedings of SPIE International Society for Optical Engineering,* Bellingham, WA, 2001.

[49] I. Kondo and T. Hamamoto, "Seismic damage detection of multi-story buildings using vibration monitoring," in *The 11th World Conference on Earthquake Engineering,* Acapulco, Mexico, 1996.

[50] Y. Kim, R. Langari and S. Hurlebaus, "MIMO fuzzy identification of building-MR damper systems," *Journal of Intelligent and Fuzzy Systems,* vol. 22, no. 4, pp. 185-205, 2011.

[51] B. H. Kim, N. Stubbs and C. Sikorsky, "Local damage detection using incomplete modal data," in

Proceedings of the 20th International Modal Analysis Conference, Los Angeles, CA, 2002.

[52] B. Xu, Z. G. Huang and S. F. Masri, "Nonparametric dynamic modeling of a non-linear frame structure with MR dampers," in *Proceedings of SPIE 2nd International Conference on Smart Materials and Nanotechnology in Engineering*, Belingham, WA, 2009.

[53] B. Liu and J. Chen, "Control system design of magneto-rheoloical damper under high-impact load," *Modern Applied Science,* vol. 5, no. 5, pp. 253-257, 2011.

[54] J. Wang and Y. Li, "Dynamic simulation and test verification of MR shock absorber under impact load," *Journal of Intelligent Material Systems and Structures,* vol. 17, no. 4, pp. 309-314, 2006.

[55] M. Ahmadian and J. A. Norris, "Experimental analysis of magnetorheological dampers when subjected to impact and shock loading," *Communications in Nonlinear Science and Numerical Simulation,* vol. 13, no. 9, pp. 1978-1985, 2007.